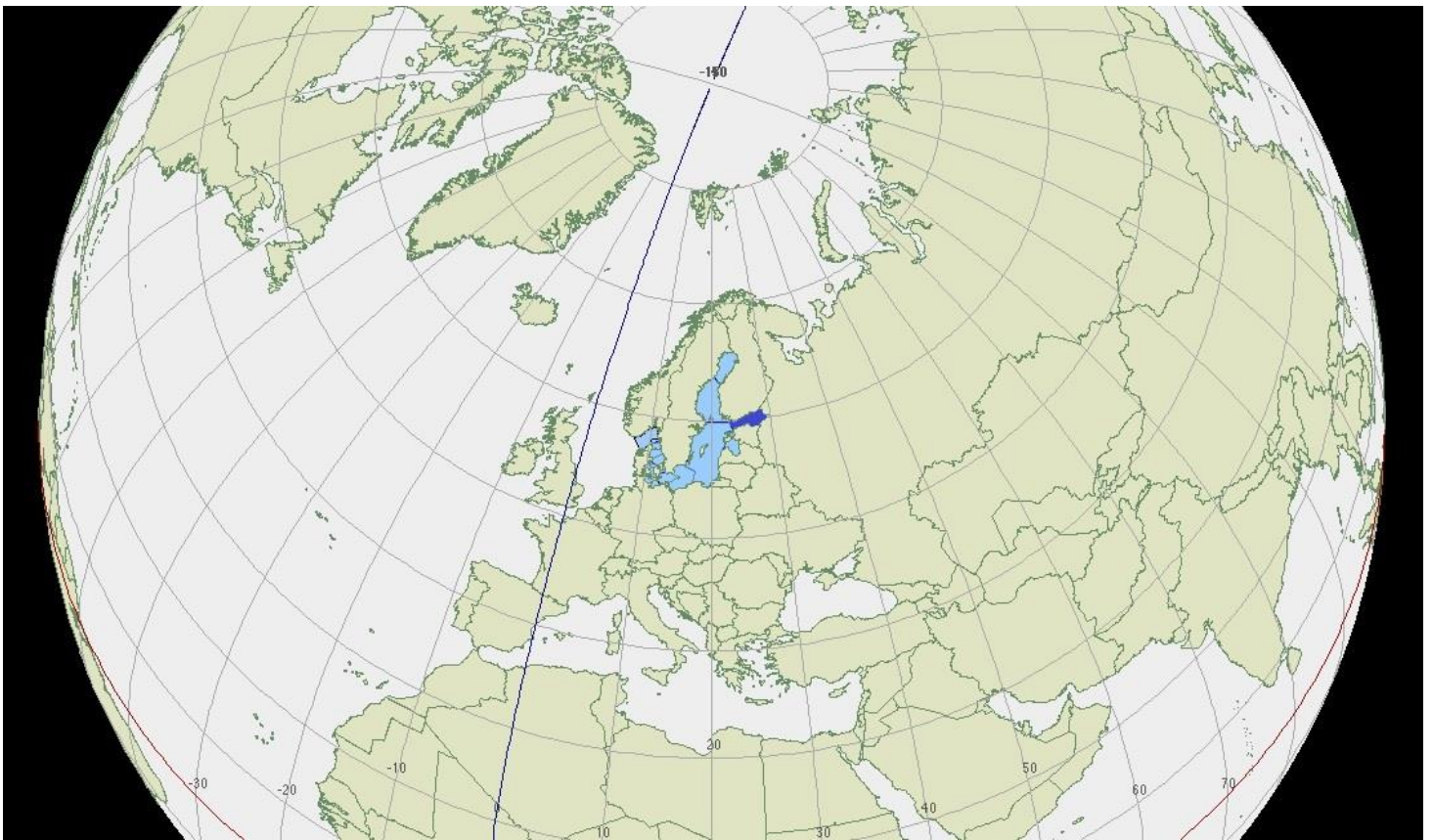


Phosphorus burial and associated sediment geochemistry in the Gulf of Finland:

the role of inter-decadal redox variability



E. van Zadelhoff
student number: 0424188
Course code: GEO4-1520

Supervisors:
Dr. Tom Jilbert
Prof. dr. ir. Caroline Slomp

Master Thesis
Department of Earth Sciences
Faculty of geosciences - Geochemistry

Utrecht University
The Netherlands

January 15, 2014

Abstract

Due to the anthropogenic loading of nutrients since the beginning of the 1900's, eutrophication related hypoxia has become a problem in the Baltic Sea. Efforts have been made to significantly reduce the anthropogenic loading but internal feedback mechanisms in the phosphorus cycle prevent a recovery to pre-industrial conditions. In recent years, several studies have been made into phosphorus cycling in the deep basins of the Baltic Sea to understand and tackle the details of this feedback mechanism. In particular, phosphorus burial in deep basin sediments has recently been better characterized. However, phosphorus burial in sediments close to the halocline has been less intensively studied.

This study investigates phosphorus burial in the Gulf of Finland, a shallow and highly eutrophied subbasin of the Baltic Sea. A large area of the sediments of the Gulf of Finland underlie halocline waters, making them susceptible to variable redox conditions. We focus on the impact of inter-decadal redox changes on sedimentary chemistry during the late 20th century, which strongly influence phosphorus burial. Bulk sediment analysis, pore water and phosphorus speciation was done on three cores taken along a transect near the halocline, where oxic to seasonally hypoxic conditions prevail. Sediment age dating (²¹⁰Pb) was done to couple sedimentary signals to bottom water oxygen data over the past 50 years. Furthermore, bottom water oxygen data from the Gulf of Finland were compared to the evolution of bottom water oxygen concentrations in the deep Baltic Proper. By doing so we link the dynamics of the shallow Gulf of Finland to the better studied deep basins of the Baltic Sea.

Although Fe-oxide bound P in the surface sediments is high, confirming large seasonal PO₄²⁻ release into the water column due to reductive dissolution of Fe-oxides, we also found high background Fe-P concentrations at these sites, which we interpret as vivianite. We found the rate of vivianite formation to be coupled to C_{org} concentrations, and therefore peaks in Fe-P occurred during periods of increased hypoxia. Similar background Fe-P concentrations have so far only been found at permanently anoxic sites. Our findings show that, not only in the deep basins but also in shallow areas close to the halocline, Fe-P can be an important long-term burial phase for phosphorus. Hence this is significant information for Baltic Sea nutrient budget calculations and models.

Contents

| | |
|--|----|
| 1. Introduction..... | 3 |
| 2. Background..... | 5 |
| 2.1 Physical oceanography of the Baltic Sea | 5 |
| 2.2 Gulf of Finland | 7 |
| 2.3 Chemical background | 8 |
| 3. Methods | 10 |
| 3.1 Study sites..... | 10 |
| 3.2 Onboard sampling and analysis..... | 10 |
| 3.3 Sediment slicing and analysis | 10 |
| 3.4 Historical water column analysis..... | 13 |
| 4. Results | 15 |
| 4.1 Redox history of the GOF | 15 |
| 4.2 Porewater chemistry | 18 |
| 4.3 Bulk solid-phase chemistry..... | 20 |
| 4.4 P-species..... | 23 |
| 5. Discussion | 24 |
| 5.1 Oxygen variability in the GOF and Baltic Proper | 24 |
| 5.2 Sediment records of redox history..... | 26 |
| 5.3 The impact of redox conditions on sedimentary geochemical cycles..... | 27 |
| 5.4 Spatial variability in redox conditions and organic matter input along the GOF transect..... | 31 |
| 5.4a Water-depth gradient..... | 31 |
| 5.4b Independent of oxygen | 31 |
| 5.5 Phosphorus..... | 33 |
| 6. Conclusions..... | 35 |
| Acknowledgements..... | 37 |
| References..... | 38 |

1. Introduction

The Baltic Sea is one of the largest brackish water basins in the World, and is characterized by the presence of a permanent halocline. This density stratification makes the Baltic Sea naturally vulnerable to bottom water hypoxia (oxygen concentrations of <2 ml/L, Conley et al., 2002), by preventing oxygenated surface water to mix with oxygen depleted bottom waters (Gustafsson and Stigebrandt, 2007). Since its formation, the Baltic Sea experienced several hypoxic intervals (Zillen et al., 2008; Jilbert et al., 2013b). However, the present day hypoxic event has intensified more rapidly and has a larger spatial extent and longer duration than any other event (Savchuck et al., 2008; Conley et al., 2009; Mort et al., 2010; Larsson et al., 1985; Rönnerberg and Bonsdorff, 2004; Gustafsson et al., 2012; Jilbert et al., 2013b).

With a catchment area in which approximately 85 million people live (Helcom, 2013), the Baltic Sea is subject to high anthropogenic loading of nutrients. Since the 1950's, anthropogenic input into the Baltic has increased 4-fold for total nitrogen and 8-fold for total phosphorus (Larsson et al., 1985, Rosenberg, 1990; Gustafsson et al., 2012).

Algal growth rates are limited by nutrient availability (Cloern, 2001), so enhanced loading of nutrients has led to excessive blooms and elevated fluxes of organic matter to the sediments (Gustafsson et al., 2012). Cyanobacteria are capable of fixing nitrogen from the atmosphere, which makes phosphorus availability the limiting factor for cyanobacteria blooms (Vahtera, 2007). After the spring bloom, nitrogen is depleted from the surface water which enables cyanobacteria to flourish during a second bloom in late summer, thereby enhancing depletion of bottom water oxygen concentrations. Additionally, phosphorus release is known to be enhanced from sediments underlying hypoxic or anoxic bottom waters due to the reductive Iron (Fe)-oxyhydroxide associated P release into the water column (Einsele, 1936; Mortimer, 1941, 1942; Conley et al., 2002) and preferential remineralization of P relative to that of carbon and nitrogen during anaerobic degradation (Ingall et al., 1993; Ingall and Jahnke, 1994; Slomp et al., 2002; Jilbert et al., 2011).

This way eutrophication has set into motion a positive feedback cycle that prevents removal of phosphate from the system through burial, leading to continuously growing problems with hypoxia and anoxia (Conley et al., 2002; Reed et al., 2011).

Bottom water anoxia causes harmful long-term consequences on ecosystem functioning. Habitat loss of benthic and fish communities (Karlson et al., 2005; Cardinale and Modin, 1999; Diaz and Rosenberg, 1995; Mackenzie et al., 2000; Karlsson et al., 2002; Diaz and Rosenberg, 2008) leading to dead sea-beds, depletion of fish stocks and toxic algal blooms (Sellner, 1997) are major problems, especially in the Gulf of Finland (HELCOM 2002; Rönnerberg and Bonsdorff, 2004). Furthermore, these problems restrict the recreational and economic use of the sea (Lukkari, 2008).

Measures have been taken to reduce the anthropogenic loading and regulate the effects of eutrophication in the Baltic (HELCOM, 2007). But despite the decline in external loading since 1980-1990 (Emeis et al., 2000, Gustafsson et al., 2012) eutrophication and the occurrence of algal blooms have not diminished, and long-term measurements of wintertime phosphate (PO₄-P) concentrations in water reveal an increasing trend over the past ca. twenty years (Olsonen 2007, Suikkanen et al., 2007, Fleming-Lehtinen et al., 2008), especially in the Gulfs of Riga and Finland (Gustafsson et al., 2012).

Phosphorus is the key nutrient in the positive feedback cycle described above, and a better understanding of its dynamics is crucial for improving water quality in the Baltic Sea. Still, its behaviour in Baltic Sea sediments has only recently begun to be studied in detail (Hille et al., 2005; Lukkari et al., 2009; Mort et al., 2010), and a large amount remains to be learned about the response of phosphorus regeneration, and burial, to spatial and temporal hydrographic variability (Jilbert et al., 2011). Additionally, knowledge is biased by the habit of focussing on deep stations (Conley et al.,

2002). Since only 10% of the bottom area is situated below a depth of 108 m, studies of the deepest sites are not representative for the entire Baltic Sea system (Conley et al., 2002).

In this study we aim to quantify the impact of redox changes on sedimentary chemistry and gain insight in the mechanisms by which phosphorus is cycled in the Gulf of Finland.

Water column data covering the past 50 years were retrieved from DAS (Data Assimilation System, at the Baltic Nest Institute at the University of Stockholm). This allowed us to reconstruct the evolution of oxygen conditions in the Gulf of Finland. We compared this with pore water and sediment data of three cores situated on the Northern slope of the Gulf of Finland (HYPER cruise, June 2009). These cores were taken along a transect of increasing depth at the halocline. Via sediment age dating (^{210}Pb), we were able to couple the sedimentary signals of redox sensitive elements (molybdenum, iron, sulfur, manganese and $\text{C}_{\text{org}}/\text{P}_{\text{org}}$) and phosphorus speciation data to water column redox changes. Our study contributes to a better understanding of the Baltic Sea environment which is necessary to restore the ecological status, as described in the HELCOM 2021 action plan (HELCOM, 2007).

2. Background

2.1 Physical oceanography of the Baltic Sea

The Baltic Sea was formed during the final stages of the last glaciation (10000B.P.). Around 8000 B.P., a sea level rise accompanied by a subsidence of sills in the Belt Sea, at the mouth of the basin, caused the environment to slowly change from a freshwater lake to a brackish sea (Sohlenius et al., 2001). This is the beginning of the formation of the Baltic Sea as we know it today. The permanent halocline is a dominant feature of the Baltic Sea, and is fundamental in influencing every other component of the system, like water column and sedimentary chemistry (Sohlenius et al., 2001).

The Baltic Sea has been characterized as a large tideless estuarine system (Elken et al., 2003) comprising several geographically and topographically defined sub-basins; Bothnian Bay (BB), Bothnian Sea (BS), Baltic Proper (BP), Gulf of Finland (GOF), Gulf of Riga (GR) (Figure 1). The Belt Sea forms the inlet, and the fact that it is relatively shallow prevents vast amounts of saline water to enter the Baltic Sea from the North Sea (Figure 2). A continuous saltwater inflow along the bottom (10-20‰) sustains the long-term halocline. The extent and direction of water flowing in and out of the Baltic is determined by pressure gradients in the Belt Sea (Wulff et al., 2001). Entrainment causes the overall salinity of the inflowing current to decrease and the volume flow to increase along the flow path (Stigebrandt, 1987; Lass and Mohrholz, 2003; Arneborg et al., 2007).

The flow path of inflowing saline water is strongly controlled by density effects, and therefore the salinity distribution follows the bathymetry (Figure 3), and leads to the formation of a permanent halocline at about 60m. The fresh water input at the surface enhances the stratification even further.

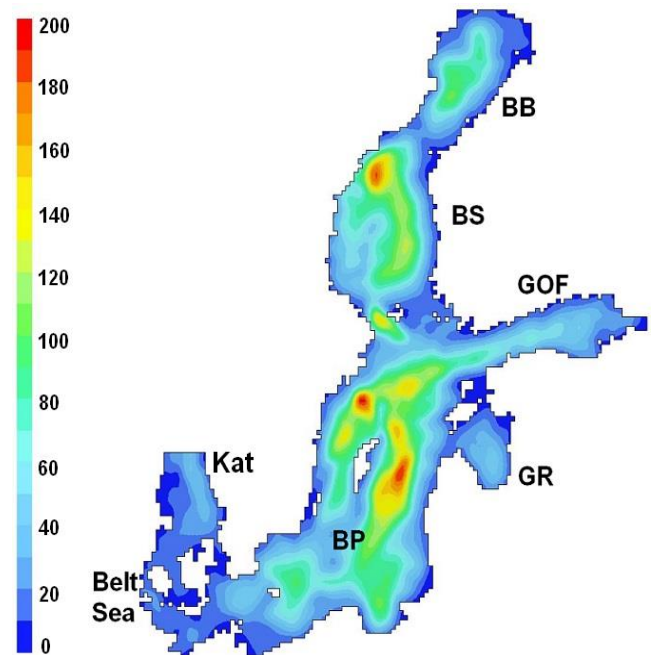


Figure 1. Bathymetric map of the Baltic Sea and its subbasins, depth scale in meters. Extracted from DAS.

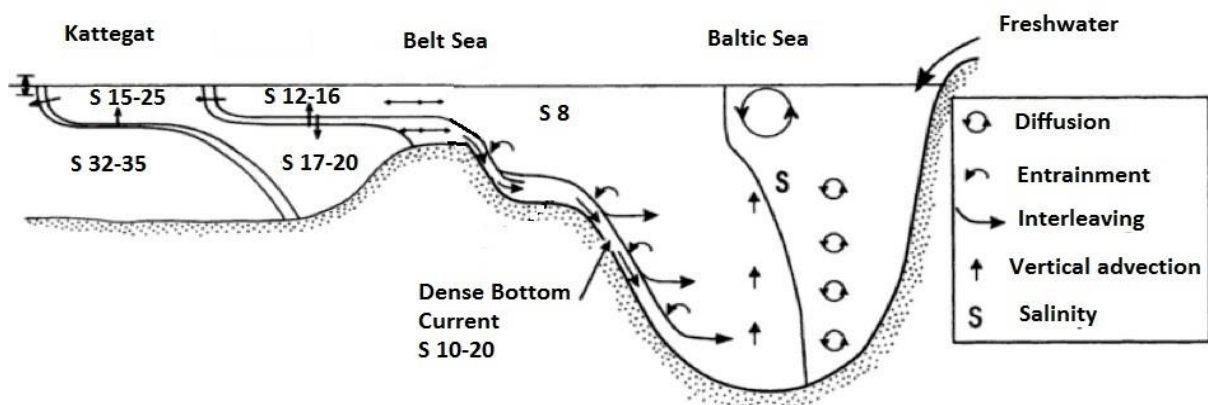


Figure 2. Salinity gradients of in- and outflowing water from the area of the mouth to the Baltic central. Surface water (~8‰) is mixed with inflowing water from Skagerrak water (~33‰), the sill depth varies between 18 and 8 meters. (Adjusted from Wulff et al, 2001).

The rapid salinity changes that occur in the Belt Sea are clearly visible in the profile shown in Figure 3. The Gulf of Riga and Bothnian Sea are less affected by salt water inflows (Figure 3), a sill at the entrance prevents saltwater to penetrate into these basins (Wulff et al., 2001). There is no sill at the entrance of the GOF basin which means it is affected by the processes that occur in the Belt Sea and the open Baltic, like major inflows.

Major inflows are events in which large volumes of highly saline water enter the Baltic over a short period of time. This happens occasionally and is a separate phenomenon from the continuous bottom inflow in the Belt Sea that usually is of lower salinity and only penetrates the waters in the Baltic Sea at intermediate depth. These inflows are associated with stormy weather conditions in the Belt Sea and when they occur, it is usually during winter months (Matthäus and Frank, 1992). It is then that these storms are strong enough to mix the entire water column in the shallow Belt Sea. Since they are weather dependent, major inflows occur irregularly and with intervals of several years (Wulff et al., 2001).

During the time interval between such major inflows, the bottom water in the deep basins of the

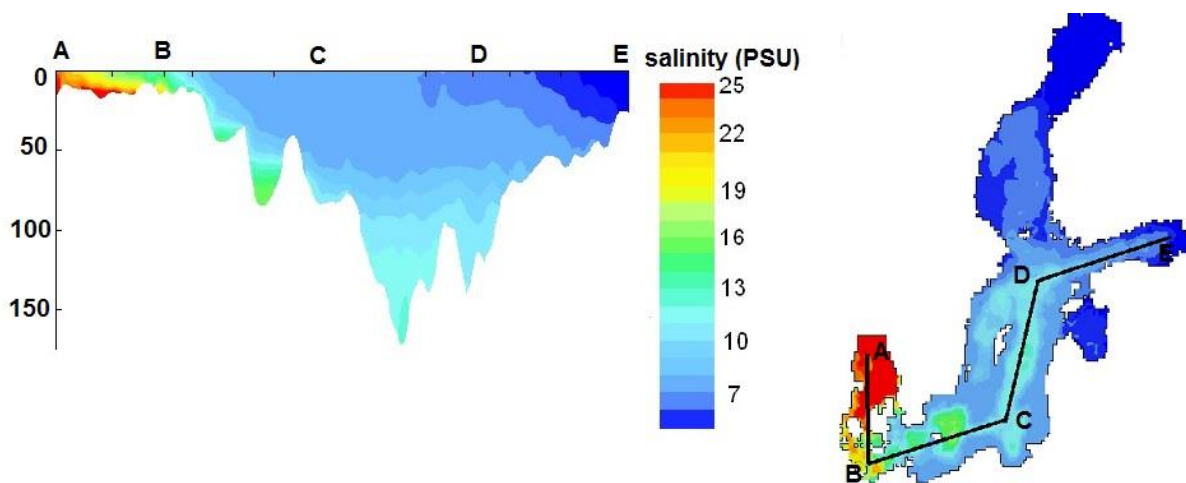


Figure 3. Salinity distribution in the Baltic Sea along a transect from the Kattegat (A) to the eastern GOF (E). Figure based on present day data retrieved from DAS (Baltic nest institute at the University of Stockholm).

Baltic Sea can be considered to be stagnant. The strong halocline limits vertical mixing, which causes the residence time of the deep water to increase roughly by a factor of five (Reissman et al., 2009). Furthermore, during stagnation periods the halocline is gradually weakened by upward diffusing saltwater, however this process is slow and the duration of these stagnation periods is usually too short for the deepest sites of the Baltic Sea to be affected.

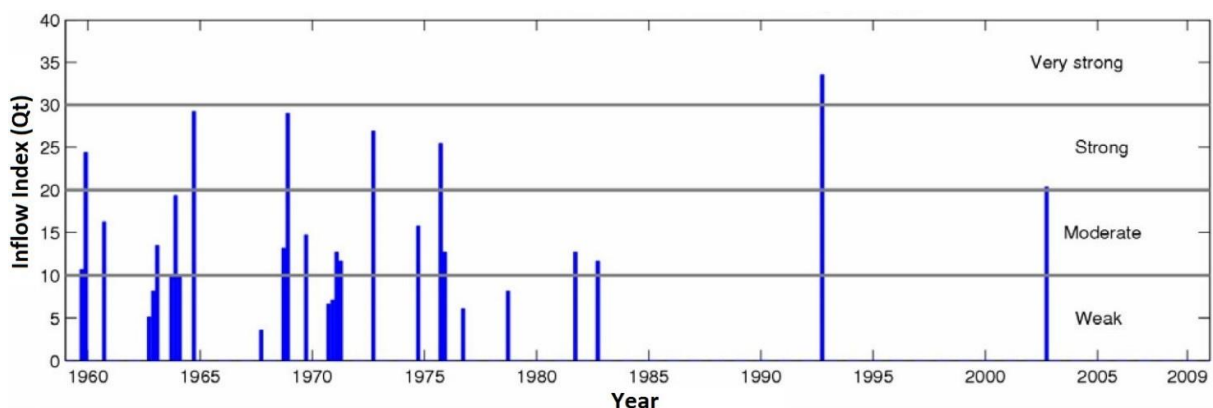


Figure 4. Intensity of inflows to the Baltic Sea 1960 – 2010 (Hansson et al., 2011), revised and updated from Matthäus and Frank, 1992.

The frequency of major salt water inflows has decreased since the early 1980's (Figure 4). Major inflows and stagnation periods significantly affect water column oxygen concentrations. A major inflow brings saline and oxygen rich waters into the deepest basins. This oxygen is quickly used up by remineralization of organic matter that rains down from the water column (Fonselius, 1969; Fonselius et al., 1984). The stratification effect that remains causes the deep waters to be decoupled from the relatively oxic surface waters, so despite a short lived increase in oxygen levels, the effect of a major inflow on the long-term is usually an intensification of bottom water anoxia. Additionally, seasonal changes can have a large effect on water column stratification. During spring and summer, a thermocline develops above the halocline at depths between 10-30m. Winter cooling and strong south-westerly winds enhance surface water mixing and break up the thermocline. The seasonal presence or absence of a thermocline, together with seasonal fluctuations in river runoff (Mattäus & Lass, 1995), can strengthen or weaken the halocline. Especially in the GOF this is significant, since it is a shallow basin that receives large amounts of freshwater.

2.2 Gulf of Finland

The GOF accounts for about 5% of the volume of the Baltic Sea (Table 1), nevertheless it receives about one quarter of the annual fresh water input into the Baltic (Alenius et al., 1998). More than half of this is delivered by the river Neva. The rivers Kymi, Narva and Luga contribute the remaining part of the freshwater input. The short water residence time and shallow depth (Table 1) are important factors for the GOF that cause rapid internal dynamics compared to the Baltic Proper. The hydrography has a typical estuarine salinity distribution (Mälkki and Tamsalu, 1985; Haapala and Alenius, 1994), characterized by large horizontal and vertical salinity variations (Figure 5). The absence of a sill between the Baltic proper and GOF in the west enables saline bottom water (9-12‰) to enter the basin easily from the West (Winterhalter et al., 1981; Meier et al., 2006; Middelburg & Levin, 2009). Fresh water of the river Neva enters the basin in the East, where salinity accounts 0-3‰.

Table 1. Hydrographic facts of the Baltic Sea and GOF

| | GOF | Baltic Sea |
|--------------------------------------|-----------------------------|----------------------------|
| Average depth (m) | 37 (Helcom, 2013) | 53 (Helcom, 2013) |
| Maximum depth (m) | 137 (Helcom, 2013) | 459 (Helcom, 2013) |
| Volume (km³) | 1100 (Alenius et al., 1998) | 21,547 (Helcom, 2013) |
| Surface area (km²) | 29.600 (Helcom, 2013) | 415,266 (Helcom, 2013) |
| Water residence time (years) | 2-3 (Alenius et al., 1998) | 32 (Wulff & Larsson, 2001) |

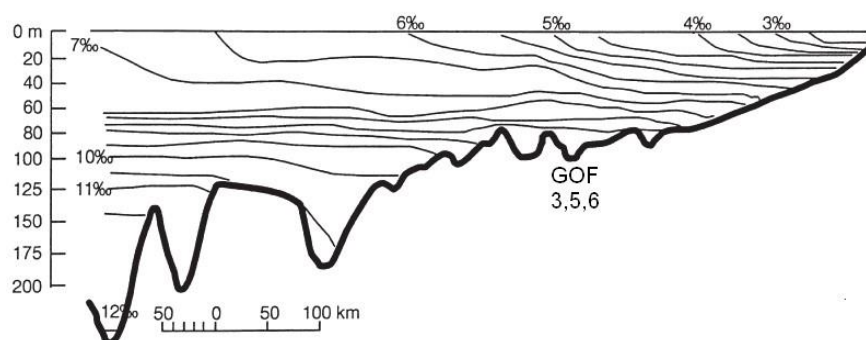


Figure 5. Typical vertical section of salinity through the GOF and Northern Baltic Sea in summer. Salinity isolines are shown as continuous lines with an interval of 0.5‰. (from Jurva, R. 1952).

Although less pronounced than in the Baltic proper, this salinity difference is large enough for a permanent halocline to be present at a depth of 60-80m throughout most of the GOF (Alenius et al., 1998; Kullenberg, 1981).

This causes the GOF to also be vulnerable to hypoxia. The circulation fluctuates between seasons (Alenius et al., 1998), and hydrographic structures are strongly influenced by wind patterns (Elken et al., 2003). Still, the general circulation pattern in the basin is anticlockwise; e.g. eastward transport along the Estonian coast and westward transport along the Finnish coast (Figure 6).

The river Neva is a major source of nutrients, since it passes through St. Petersburg before it enters the GOF. This makes the GOF one of the most heavily eutrophied subbasins of the Baltic sea with an external nutrient load of 2–3 times the average for the Baltic Sea (Pitkanen et al., 2001, Rönnerberg & Bonsdorff, 2004). Therefore, waters passing the Finnish coast have experienced a build-up of nutrients, since it has been contaminated by inflowing waters of the river Neva.

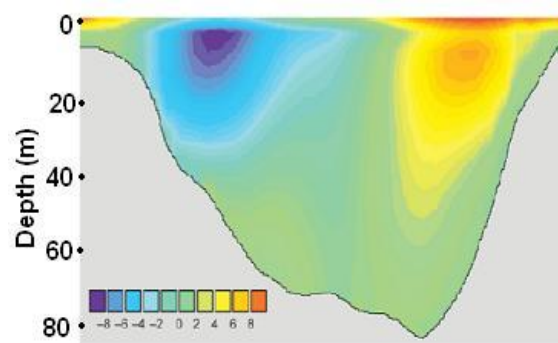


Figure 6. simulated five year means of inflow (positive) and outflow (negative) in cm/s at the entrance of the Gulf, figure from Andrejev et al., 2004. Northern slope left, Southern slope right.

2.3 Geochemical processes in marine sediments

Sediments are mainly composed of inorganic material (mineral particles) which may have a detrital or biogenic origin. However, organic matter is the driving force for ‘early diagenesis’, and can be defined as the combination of processes that occur in the sediment after deposition which alter the composition of the sediment and porewaters.

Organic matter remineralization is catalyzed by bacterial respiration, from which bacteria acquire energy for metabolism. The occurrence of specific respiratory processes is thus controlled by the free energy yield per mole of organic carbon oxidized by each of a series of electron acceptors (Claypool and Kaplan, 1974; Froelich et al., 1979). Aerobic respiration uses oxygen as the electron acceptor and is the most efficient respiratory process in terms of energy acquired per mole of carbon oxidized (table 2). When oxygen is depleted, suboxic and anoxic redox reactions become the dominant pathways by which organic matter is remineralized. The succession of redox reactions leads to a chemical zonation in the sediment where O_2 , NO_3^- , bioavailable Mn(IV) and Fe(III) and SO_4^{2-} diminish successively with depth. Reduced products of these reactions are NH_4^+ , Mn^{2+} , Fe^{2+} , HS^- and CH_4 , which are produced successively with depth (Froelich et al, 1979), as shown in table 2.

Table 2. Successive terminal electron acceptors used in organic matter remineralization and their free energy standard state (25 °C, 1atm). Values of standard free energies of formation are from Stumm and Morgan (1996).

| Process | Chemical reaction | ΔG° (kJ mol glucose ⁻¹) | % relative energy efficiency |
|---------------------|---|--|------------------------------|
| Aerobic respiration | $C_6H_{12}O_6 + 6O_2 \rightarrow 6H_2O + 6CO_2$ | -2.82 | 100 |
| Denitrification | $5C_6H_{12}O_6 + 24NO_3^- \rightarrow 12N_2 + HCO_3^- + 6CO_2 + 18H_2O$ | -2.66 | 94 |
| Manganese reduction | $C_6H_{12}O_6 + 18CO_2 + 6H_2O + 12MnO_2 \rightarrow 12Mn^{2+} + 24HCO_3^-$ | -2.38 | 84 |
| Iron reduction | $C_6H_{12}O_6 + 42CO_2 + 24Fe(OH)_3 \rightarrow 24Fe^{2+} + 48HCO_3^- + 18H_2O$ | -0.79 | 28 |
| Sulfate reduction | $C_6H_{12}O_6 + 6SO_4^{2-} \rightarrow 6H_2S + 12HCO_3^-$ | -0.48 | 16 |
| Methanogenesis | $2C_6H_{12}O_6 \rightarrow 6CH_4 + 6CO_2$ | -0.30 | 11 |

Changes in external influences cause non-steady state conditions in the sediment which can result in alterations in sedimentary signals over time. Important examples of such external influences are bottom water oxygen content, sedimentation rate or organic matter flux to the seafloor (Kasten et al., 2004). In high productivity regions like the Baltic Sea, where organic matter input to the sediment exceeds oxygen availability, porewater O_2 is completely consumed within several millimetres to centimetres below the sediment-water interface (Cai and Sayles, 1996). Changes in bottom water oxygen concentrations therefore significantly affect the occurrence of specific remineralization reactions in the sediments of the Baltic Sea. Anoxic respiration, especially sulfate reduction, is the dominant reducer of organic matter in these sediments. Remineralization reactions release ions into the porewater, as well as the reduced products listed above. With the production of CO_2 or HCO_3^- , a change in pH conditions in the porewater occurs. The altered chemistry catalyses many processes, such as authigenic mineral formation. Authigenic minerals are formed in situ and play an important role in geochemical cycling of Fe, S and Mn. Additionally they can form a sink for reactive P.

Iron plays an important role in many processes involving authigenic mineral formation. About 60% of sedimentary iron is captured in the form of silicates (Habricht and Canfield, 1997; Chester, 2000; Thamdrup, 2000), and behaves unreactive. Only a small fraction of the silicate bound iron (12-26%) can be reduced during weathering (Thamdrup et al., 2000), thereby releasing reactive iron (Fe^{2+}). Under oxic conditions, Fe^{2+} ions (and Mn^{2+} ions) can precipitate as oxides (thereby forming Mn-oxides and Fe-oxides). Fe-oxides have a very high affinity for the adsorption of anions as well as cations under natural conditions the early diagenetic reactivity of iron is often of great significance for the behaviour of compounds such as trace metals, phosphate and organic acids. Fe-oxides are vulnerable to reductive dissolution when oxygen becomes depleted, thereby releasing PO_4^{2-} and Fe^{2+} into the water column. Consequently, phosphorus cycling in coastal and continental margin sediments such as the Baltic Sea, is strongly coupled to iron redox cycling (Krom and Berner, 1981; Klump and Martens, 1987; Sundby et al., 1992; Jensen et al., 1995; McManus et al., 1997; Slomp et al., 1996b).

Under anoxic conditions, Fe^{2+} can react with hydrogen sulfide (H_2S) to form metastable sulfide (FeS) and pyrite (FeS_2). Therefore iron and sulfur cycles are closely coupled in sediments subject to fluctuating redox conditions. In a basin like the Baltic Sea, a shift towards more reducing conditions can cause Fe-oxides near the redoxcline to dissolve. The Fe^{2+} that is released can become transported to deeper euxinic waters where oxygen is absent and dissolved sulfide (H_2S) is present in the water column. This process of remobilization, transportation and precipitation of reactive iron is called shuttling and leads to reactive iron enrichments in deep euxinic basins (Lyons and Severmann, 2006). Strongly elevated ratios of highly reactive iron to total iron ($Fe_{Reactive}/Fe_{Total}$) and total iron to aluminum (Fe_{Total}/Al) and high degrees of pyritization (DOP) are each products of this enrichment process and can therefore be used as paleoredox proxies of euxinia (Berner, 1970; Canfield, 1989; Lyons and Severmann, 2006). Another sedimentary paleoredox proxy molybdenum, which is scavenged by FeS and organic matter under sulfidic bottom water conditions (Helz et al., 1996). Furthermore, due to the preferential regeneration of phosphorus from organic matter under low-oxygen conditions, C_{org}/P_{org} ratios can also be considered as a redox proxy.

The PO_4^{2-} that is released into the porewater from the reduction of iron oxides or organic matter can precipitate in situ as vivianite ($Fe_3(PO_4)_2 \cdot 8H_2O$). Vivianite is an authigenically formed mineral and since it is unreactive to reducing conditions, it can form a long term burial phase for P. Vivianite is typically known to precipitate below the sulfur-methane transition (SMTZ), where concentrations in the porewater are high in Fe^{2+} (Bray et al. 1973) and dissolved PO_4^{2-} (März et al., 2008). Under these conditions supersaturation with respect to vivianite may be reached. However, recent findings by Milucka et al. (2012) provide evidence for a potential biogenic vivianite formation within the SMTZ. They observed intracellular precipitates of Fe(II) phosphate within cells of *Desulfosarcina* (DSS) bacteria.

3. Methods

3.1 Study sites

Three cores were sampled in May 2009 along a transect on the Northern slope of the GOF (Figure 7) as part of the HYPER/COMBINE cruise of the R/V *Aranda*. The cores were taken along a gradient of increasing depth; GOF3 (25.3234°E, 60.07380°N) at 59m, GOF5 (25.18383°E, 59.95165°N) at 64m and GOF6 (25.10968°E, 59.94932°N) at 70m water depth. Water column measurements (Figure 7c) show the decrease in oxygen abundance from 40m to 60m and the inverse relation with salinity, indicating the cores are situated near the halocline. Using data from cores taken at different water depths, we can investigate the effect of bottom-water oxygen conditions on sediment chemistry. However, although the study sites are situated within close distance of each other (~15km), sedimentation and erosion rates can influence the local chemistry, independent of oxygen. Such variations are caused by very local bathymetry, and it should be noted that the transect Figure 7b has too low resolution to show such specific details for each location. (Note the horizontal salinity gradient below the halocline at about 60m depth; the lower salinity on the Southern slope is displaying the anticlockwise circulation).

3.2 Onboard sampling and analysis

The sediment cores were retrieved using a multi-corer and stored with at least 10 cm of water on top to prevent oxidation (Figure 8). After coring, porewater oxygen concentrations were measured with a Unisense 100 electrode inserted into the sediment. 100% saturation data were estimated by immersing the electrode in aerated ultraclean water. Porewater samples were then collected on board by rhizons (Seeberg et al., 2005). Porewater analysis was done spectrophotometrically for NO₃, NH₄ and H₄SiO₄ by autoanalyser, and for SO₄ by ion chromatography. Parallel sub-cores were kept frozen at a temperature of -20°C until further analysis in Utrecht.

Water column measurements were taken for each coring location. Bottom water pressure, temperature [°C], salinity (ppt) and oxygen were measured with the use of a CTD-system (conductivity, temperature and density) to which an oxygen sensor was attached.

3.3 Sediment slicing and analysis

Sediment work was conducted in the laboratory at Utrecht University. Slicing of the cores was done with 0.5 - 1 cm resolution for the top 2-3 cm, followed by 2 cm thick slices below. GOF3 was sliced in a N₂-purged glove box after thawing. Because the outer part of the core collapsed, only the centre of the core was sampled. GOF3 also compacted during this procedure; the original length was reconstructed assuming linear compaction. GOF 5 and GOF 6 were sliced by a rock saw while frozen and immediately stored in bags in the freezer to prevent melting and oxidation.

The samples were freeze-dried (-80°C), upon which the porosity was determined by weight loss for GOF5 and GOF6. The sediment was then powdered in an agate mortar inside an N₂ purged glovebox and split into oxic and anoxic fractions. From the oxic fraction, the inorganic carbon content was determined through decalcification of 0.5 grams of sediment in 10ml HCl [1M] solution (Van Santvoort et al., 2002) and put in the shaker for 12 hours. Fluid with dissolved carbonate was extracted into a Greiner tube. This was repeated by a second rinse of 4 hours after which the samples were put in the oven overnight to dry (60°C). After decalcification the organic carbon fraction was determined by combustion using an elemental analyser (Fisons NA 1500 NCS, precision and accuracy <2% based on an atropine/acetanilide standard calibration and checked against internal laboratory standard sediments).

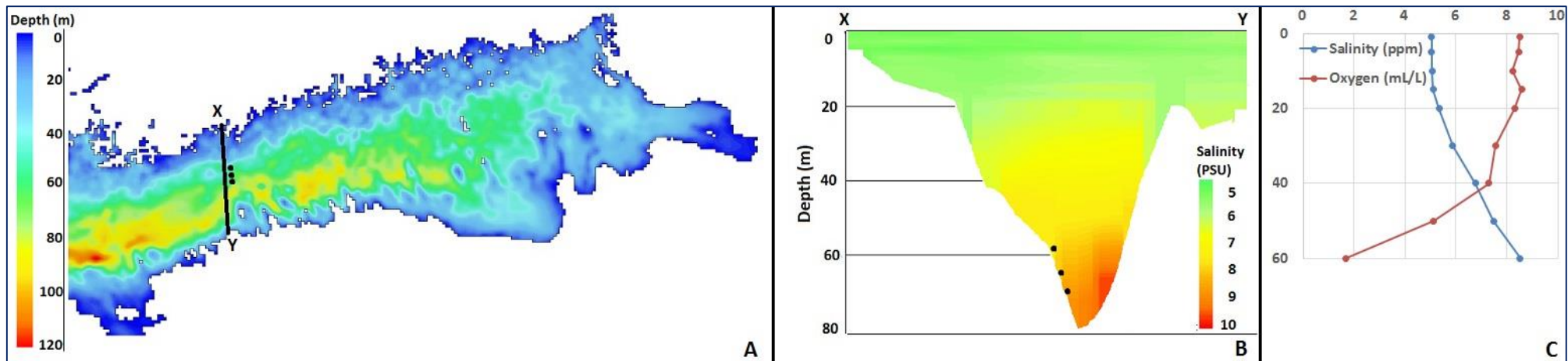


Figure 7. a. Bathymetric map of the GOF with X-Y transect of the cores GOF3-5-6. b. Salinity cross-section along the X-Y transect, extracted from DAS averaged from 1970-2010. The location of the cores are indicated at depth c. Plot of water column oxygen/salinity CTD data at GOF6 taken during the HYPER cruise may 2009.



Figure 8. photo's taken on board the ship of cores (left to right): GOF3, GOF5 and GOF6.

From the anoxic fraction, the solid phase P fractionation was retrieved using the sequential chemical extraction (SEDEX) procedure developed by Ruttenberg (1992), as modified by Slomp et al., 1996. Details on this 8-step procedure are given in Table 3. Duplicates and internal standards were included in the extraction series to assure accuracy and reproducibility. The SEDEX procedure separates total sediment P into: exchangeable P, iron oxyhydroxides (Fe-bound P), authigenic P (carbonate fluorapatite (CFA), biogenic hydroxyapatite and CaCO₃-bound P); detrital P and organic P (Table 3).

In step 2 of SEDEX (Table 3), CDB extractable Mn and Fe are a measure of the Mn oxides (Canfield et al., 1993) and Fe oxides in the sediment. It should be noted that CDB may also extract some Fe from clay minerals and from Fe sulphides (Slomp et al., 1996). The Fe and Mn concentrations in the CDB solutions of the P-extractions were measured using ICP-OES (Inductively Coupled Plasma – Optical emission spectrometry).

Sediments were shielded from oxygen until step 3 of the SEDEX procedure to avoid conversion of CFA to Fe-oxyhydroxide-bound P due to pyrite oxidation upon oxygen exposure (Kraal et al., 2009). Phosphate in all rinses was analysed colorimetrically by the ammonium heptamolybdate– ascorbic acid method (precision and accuracy <2%, based on calibration to standard solutions and checked against internal laboratory standard sediments), with the exception of the CDB rinse, in which P was analysed by ICP-OES.

The total elemental content of the sediments was determined by analysis with ICP-OES. Firstly, 0.1 gram of sediment was dissolved in 2.5 ml HF (40 %) and 2.5 ml of a HClO₄/HNO₃ mixture, in a closed Teflon bomb at 90°C for 12h. The acids were then evaporated at 190°C and the resulting gel was dissolved in 1M HNO₃, which was analysed for elemental concentrations by ICP-OES (precision and accuracy <5%, based on calibration to standard solutions and checked against internal laboratory standard sediments). The Mn content in the CDB and total destruction was unreliable for the peak values at GOF3 and at the surface of GOF5, where the detection limit was exceeded (100-200 times higher than the standard solution).

Age dating of the sediment by ²¹⁰Pb α -spectrometry was performed at NIOZ (Texel) on core GOF5 and GOF6, in order to correlate sediment depth to time. The sediment was spiked with ²⁰⁹Po and digested in 10 ml concentrated HCl in a microwave oven for 3 hours. 2 ml 3.5% HClO₄ was then added and the acids were removed by evaporation. The resulting precipitate was re-dissolved in 5 ml concentrated HCl for 30 min. Thereafter, 40 ml 0.5 M HCl (with 12 g l⁻¹ boric acid), 4 ml NH₄OH and 5

Table 3. Stages of the SEDEX sequential extraction procedure (Ruttenberg, 1992). Expected extracted phosphorus phases are listed, with references. (Table copied from Jilbert et al., 2013a).

| Stage and code | Extractant | pH | Rinsing time (h) | Expected P phases | References |
|----------------|--------------------------------------|-----|------------------|--|------------------------|
| 1 Ex-P | 1 M MgCl ₂ | 8 | 0.5 | Exchangeable, loosely sorbed P | |
| 2 CDB-P | Citrate-dithionite-bicarbonate (CDB) | 7.5 | 8 | Fe oxyhydroxide-bound P Vivianite | Nembrini et al. (1983) |
| 3 (CDB-P) | 1 M MgCl ₂ | 8 | 0.5 | Any P resorbed during stage 2 | |
| 4 Acetate-P | Na acetate buffer | 4 | 6 | Carbonate fluorapatite (CFA) Hydroxyapatite Ca-rhodochrosite-P | Suess (1979) |
| 5 (Acetate-P) | 1 M MgCl ₂ | 8 | 0.5 | Any P resorbed during stage 4 | |
| 6 Detrital-P | 1 M HCl | 0 | 24 | Detrital apatite minerals | |
| 7 | (ashing at 550 °C for 2 h) | | | | |
| 8 Organic P | 1 M HCl | 0 | 24 | Organic P | |

ml 40 g l⁻¹ ascorbic acid (in 0.5 M HCl) were added. Po isotopes were deposited by suspending silver disks in the solution, which was heated to 80°C for 4 hours then left overnight at room temperature. The activity of ²¹⁰Po was measured by α -spectrometry with Canberra Passivated Implanted Planar Silicon (PIPS) detectors, allowing ²¹⁰Pb activity to be backcalculated. 1σ counting uncertainty was on average 5 %.

With a half-life of 22.3 years, ²¹⁰Pb is a suitable radiogenic isotope for the dating of undisturbed sediments in which changes have occurred within the last century. The age vs. depth profile of the sediment was reconstructed according to the following formula, assuming a constant rate of supply of ²¹⁰Pb (CRS-model):

$$C = C_0 * e^{-km/r}$$

where C is total ²¹⁰Pb, C₀ is excess ²¹⁰Pb (background: GOF5 of 35.2 mBq/kg, for GOF6 79.7 mBq/kg), k is the decay constant (²¹⁰Pb = 0.03114), m is cumulative dry mass [cm³], and r is the dry mass accumulation rate [cm³/yr].

3.4 Historical water column analysis

To be able to place the sedimentary signals we find in the GOF in the context of the redox evolution in the Baltic Sea, we used water column data that was retrieved from the Baltic Environmental Database (BED), housed at the Baltic Nest Institute (BNI) at the University of Stockholm. The software package Data Assimilation System (DAS) was used, which is a tool to query and analyse hydrographic and chemical data from the Baltic Sea, and is coupled to BED. The database contains data on temperature, salinity and chemical concentrations of the water, based on measurements gathered throughout the Baltic. First recordings originate from around 1900. Since the 1950's data is consistent and densely spread. The database is continuously expanding by present day measurements. For the GOF, water column oxygen and salinity data for depths of 60 and 70m for 1955 to 2009 were used, collected within the area indicated in Figure 8.



Figure 8. Coördinates of the area in the GOF from which water column data were extracted.

From the selected area in the GOF (**Figure 8**), for each depth the total oxygen counts and their distribution over the years are shown in **Figure 9**. This provides information on the reliability for the interpolated monthly signal, which was based on the total oxygen counts per year.

Bottom water oxygen data from the deepest sites in the Baltic Proper (BY15, BY29, BY31, F80), were only taken from these 4 stations (**Figure 11**). The data are plotted based on a yearly average, taken from a number of observations over that year (**Table 4**).

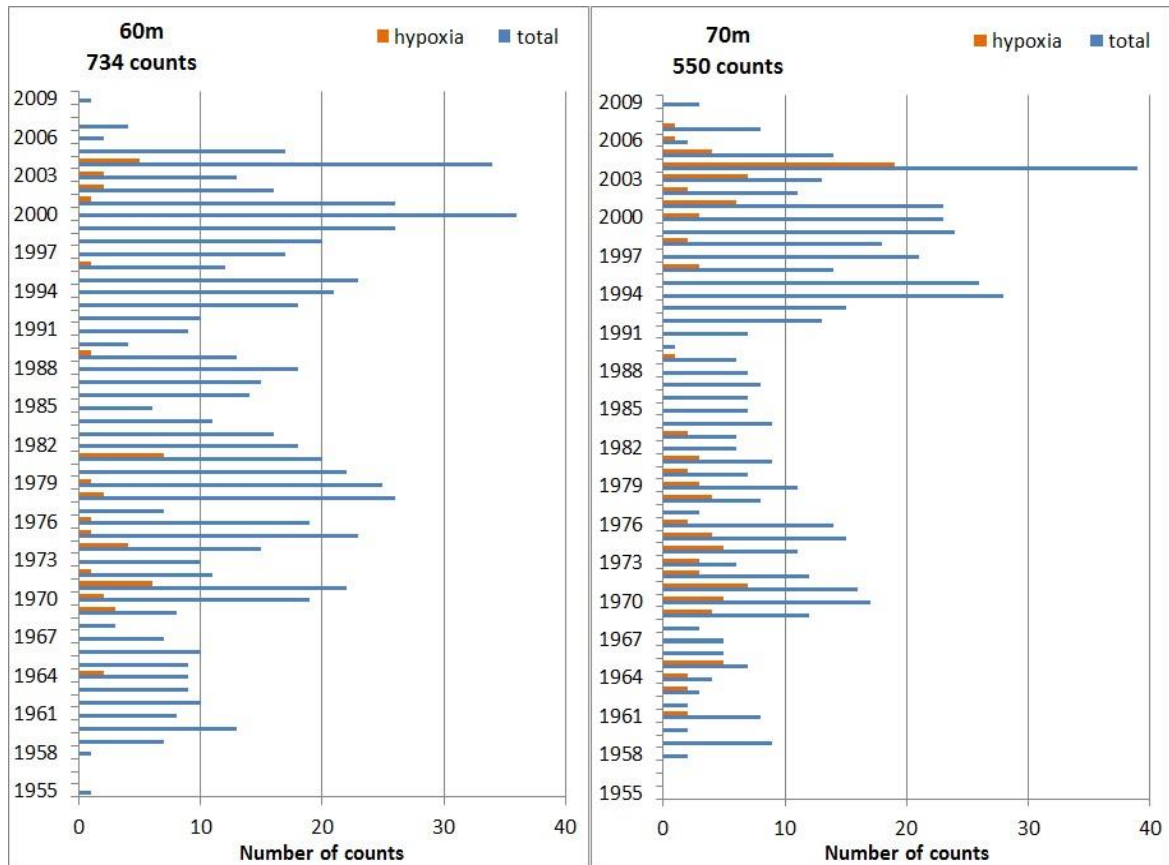


Figure 9. Total oxygen counts (blue) and hypoxia counts (orange) in the area in the GOF indicated in Figure 8 at 60m and 70m depth from 1955 – 2009.

Table 4. Average, minimum and maximum number of oxygen measurements for four sites in the Baltic

| Site | Average nr. of observations/year | Minimum nr. of observations/year | Maximum nr. of observations/year |
|------|----------------------------------|----------------------------------|----------------------------------|
| BY29 | 11 | 5 | 26 |
| BY15 | 31 | 7 | 204 |
| BY31 | 24 | 4 | 71 |
| F80 | 16 | 6 | 49 |

4. Results

4.1 Redox history of the GOF

Bottom water oxygen concentrations in the GOF over the past half century are plotted in Figure 10. The decadal trend both at 60m and 70m shows relatively constant bottom water oxygen concentrations from 1960-1975. In this period, average concentrations are 5ml/l and 3 ml/l at 60 and 70 m depth, respectively. From the mid 70's there was a slow increase over a period of about 20 years which was terminated by a major inflow in 1993 (Schinke and Matthäus, 1998). In this period (1975 to 1993), average concentrations increased to 6-7 ml/l and 5-6 ml/l at 60 and 70m, respectively.

After the inflow of 1993, bottom water oxygen concentrations show a relatively quick decrease until the second inflow in 2003 (Feistel et al., 2003) again raises oxygen levels. The yearly trend shows that this second major inflow raised bottom water oxygen levels significantly. This effect is opposite to the inflow of 1993, which caused an overall decrease in bottom water concentrations in the years that followed. The range of variation in the decadal signal is largest at 70m (Figure 10).

The salinity profile is inversely related to that of oxygen, with minimum values observed at the 1993 inflow. At this time salinity was at its lowest point since 1955, at around 6‰. This is similar to the surface water salinity (Figure 10), indicating an absence of a halocline and a complete ventilation of the water column. After the inflow salinity increased until the second major inflow in 2003, which caused a decrease in salinity.

The seasonal oxygen concentrations show large variability. The difference between summer and winter can reach 6ml/l, while the absolute variability over the complete time series is no more than 9 to 10 ml/l (Figure 10). Sub-zero oxygen concentrations are never reached at any depth. However, at 70m depth concentrations often approach and occasionally reach zero in the low oxygen periods, which is never the case at 60m depth. Maxima around 9-10 ml/l can be found both at 60 and 70m, depth. Hence, although minimum oxygen concentrations are generally depth dependent, i.e. the greater the depth, the less oxygen is present, the seasonal cycle is very important to determining the oxygen concentration at any given time.

The bottom water oxygen concentrations of four sites in the Gotland Basin are plotted in Figure 11, and again the inflows of 1993 and 2003 are indicated. All sites are hypoxic, with average values below 2ml/l. BY15 (Gotland Deep) has the lowest oxygen concentrations, and concentrations at BY31 and BY29 are highest. Values at F80 are intermediate. There is an increase in oxygen concentrations at all sites in response to both inflows.

BY15 shows some differences in oxygen response compared to the other sites. It is the second deepest site, but most anoxic. The oxygen response to the inflows at this site is delayed by about 1 year, which is unexpected since it lies further south than BY29 and BY31 where this delay is not visible. During the stagnation period from 1980-1993, oxygen levels at BY31 and BY29 show no change and keep fluctuating around zero, while at F80 and BY15 oxygen concentrations decrease to sub-zero. However, at F80 oxygen levels stabilize at around -2ml/l, whereas BY15 keeps decreasing.

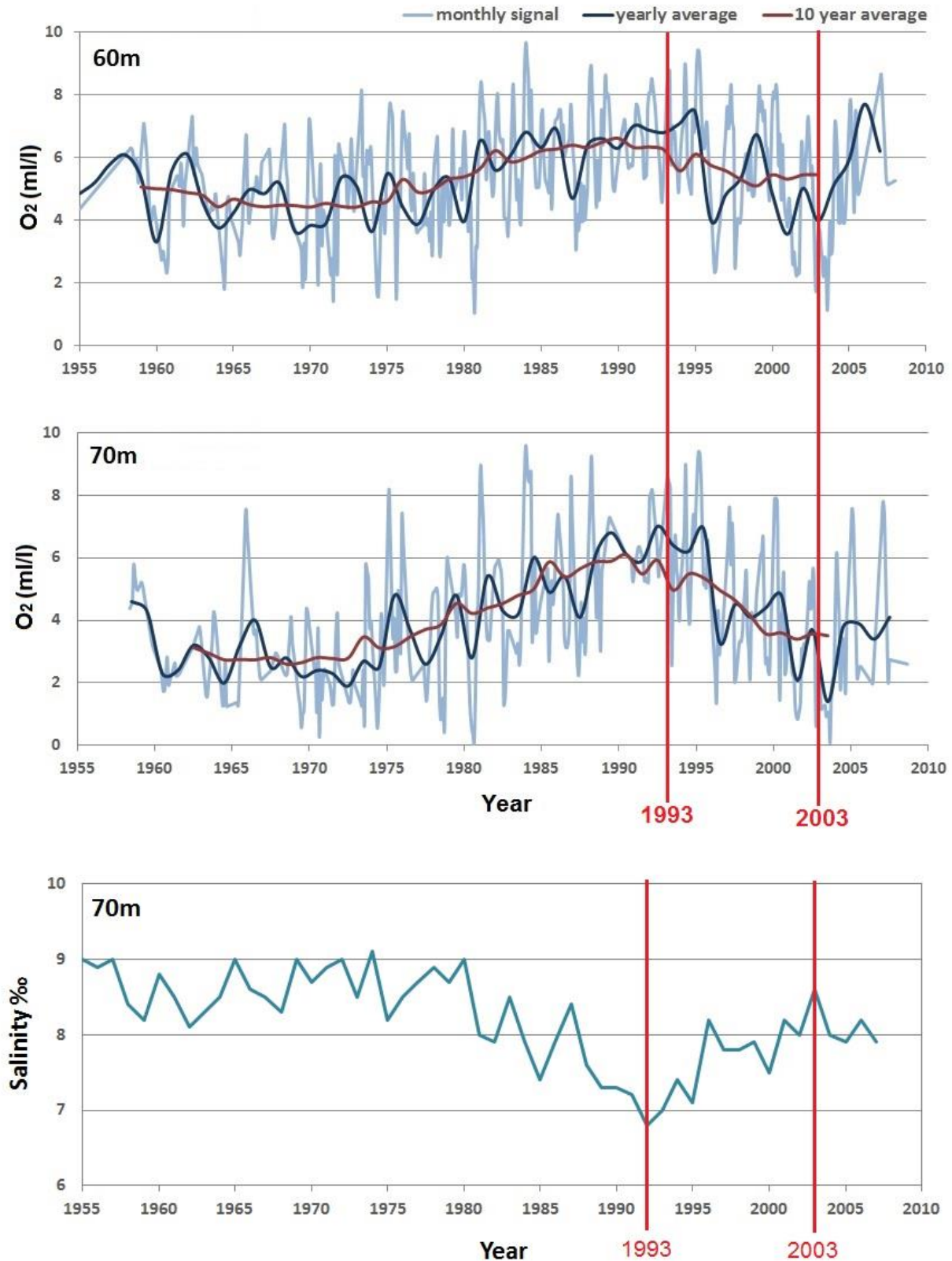


Figure 10. GOF bottom water oxygen (ml/l) and salinity (‰) time series at 60m and 70m depth at the transect. Indicated in red are the major inflows from 1993 and 2003. Monthly bottom water oxygen and monthly salinity data was obtained from Baltic Environmental Database at Stockholm University. Monthly salinity was averaged to a yearly signal. Monthly oxygen was averaged to yearly (dark blue) and decadal (dark red) signal.

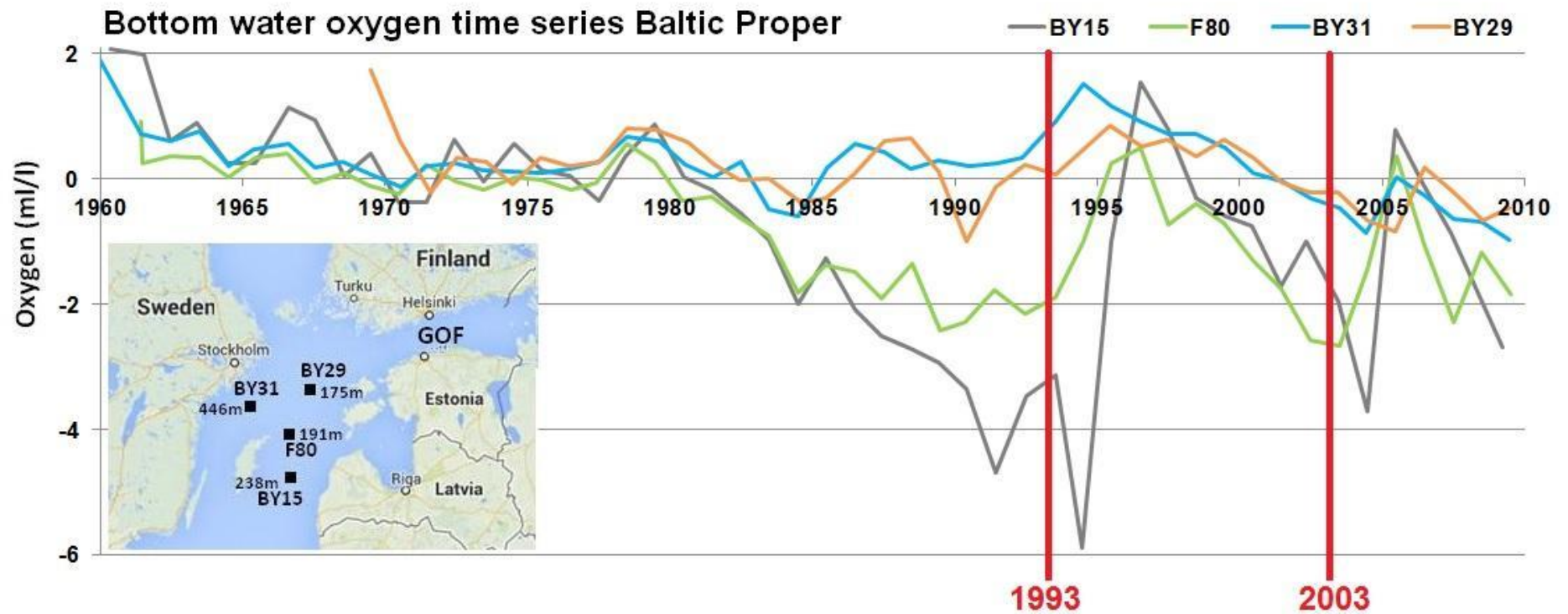


Figure 11. Bottom water oxygen concentrations (ml/l) over the period 1960-2010 (yearly) in the Baltic Proper at sites: BY15 (Gotland Deep), F80, BY29 (Northern Gotland) and BY31 (Landsort Deep). Negative oxygen concentrations are estimated from hydrogen sulfide concentrations using the molar ratio of $H_2S:2O_2$ (see Fonselius, 1981). Inflows of 1993 and 2003 indicated in red, site locations and depth are indicated on the map. Data was retrieved from Baltic Environmental Database, Stockholm university.

4.2 Porewater chemistry

Porewater oxygen concentrations at the surface sediment, and oxygen penetration depth, decrease with increasing water depth (Figure 12). From 30 $\mu\text{mol/l}$ to 1 cm at GOF3, 20 $\mu\text{mol/l}$ to 0.5cm at GOF5 and 8 $\mu\text{mol/l}$ to <0.5cm at GOF6, although the exact penetration depth at the latter site is difficult to interpret from the profile. It was difficult to make a sediment-water interface estimate, and at GOF6 this is reflected in the elongated oxygen profile. Therefore these oxygen profiles should be seen as an indication. Note that oxygen concentrations at the surface are above zero at all sites as described in the methods.

Fe^{2+} concentrations at the sediment surface are zero at all sites. At GOF3 and GOF5 there is a peak just below the surface, after which concentrations become zero at greater depth. At GOF6 a near surface peak is absent; concentrations are zero and remain so over the whole depth interval.

In contrast to Fe^{2+} , surface concentrations of Mn^{2+} range between 20 and 90 $\mu\text{mol/l}$. At GOF3 and GOF6 there is a distinct peak at the redox boundary just below the surface. The Mn^{2+} profile of GOF3 shows a second maximum at depth, whereas the profiles at the other two sites are near vertical with depth.

HPO_4^{2-} increases from the top of the sediment at GOF6, whereas at GOF3 and GOF5 concentrations only build up below a few centimetres depth. At all sites, SO_4^{2-} profiles approximately mirror HPO_4^{2-} . NH_4^+ profiles show an increase with depth at all three locations.

General differences in porewater profiles between the cores are the lower total concentrations and the lower gradients for Mn^{2+} , HPO_4^{2-} and NH_4^+ at GOF5 compared to GOF3 and GOF6. Also SO_4^{2-} decreases less steeply at GOF5; a minimum is reached at 25cm but concentrations never reach zero, whereas at the other sites concentrations reach zero concentration within 10-15cm.

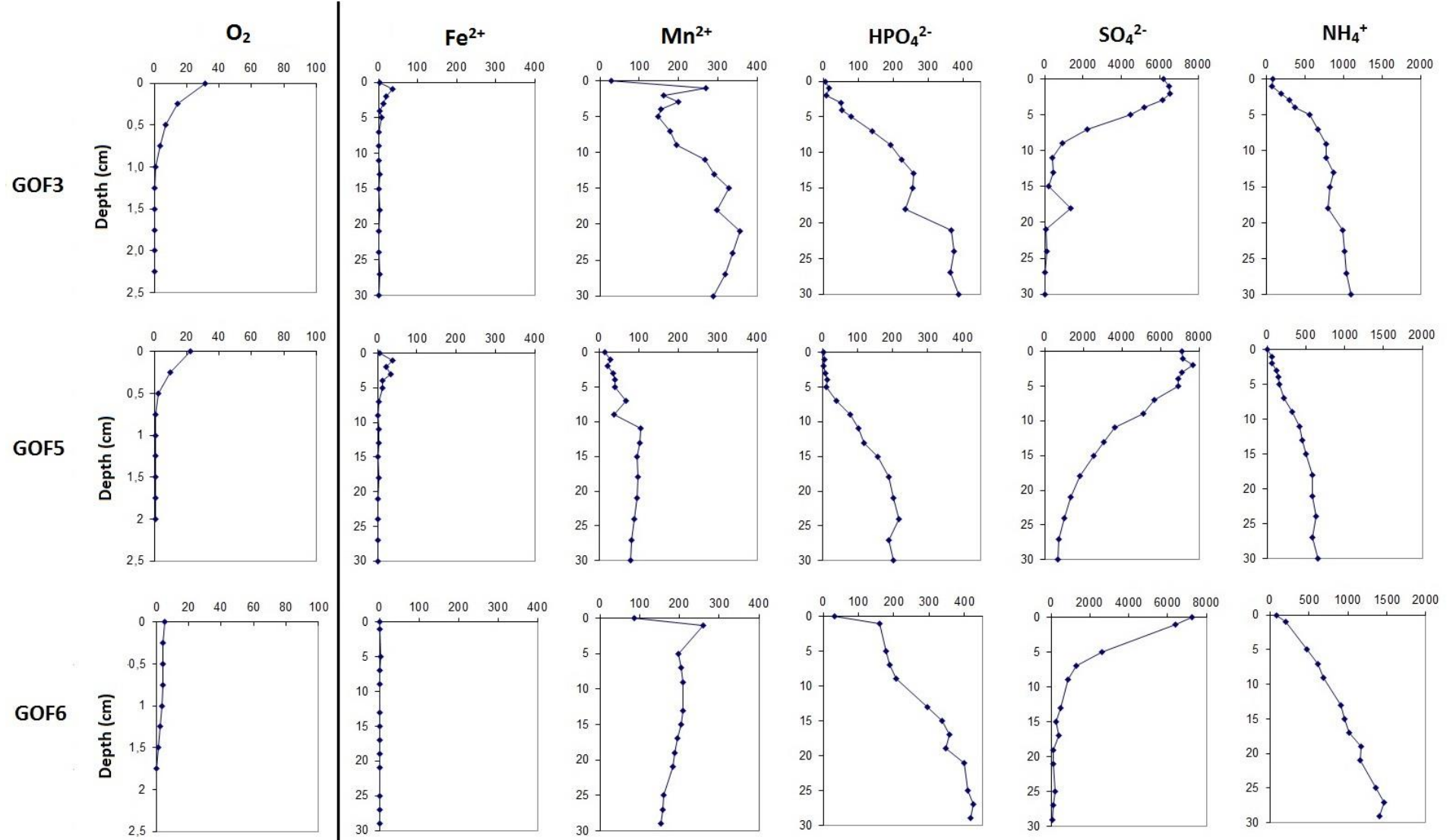


Figure 12. Porewater profiles of dissolved O_2 ($\mu mol/l$), Fe^{2+} , Mn^{2+} , HPO_4^{2-} , SO_4^{2-} and NH_4^+ (in $\mu mol/l$) at GOF3, GOF5 and GOF6.

4.3 Bulk solid-phase chemistry

At all sites, organic carbon (C_{org}) content at the surface is between 5 and 7 %wt (Figure 13), with a background value of 2%wt. At all three sites there is a decreasing trend from top to bottom. At GOF5 and GOF6 C_{org} concentrations also fluctuate at middepth, with peaks at 12cm and 30cm in these two cores, respectively. Total C_{org} content in the sediment is lowest at GOF5. Here, the vertical gradient in C_{org} is steep and the background value is reached at 18cm depth, whereas at GOF3 and GOF6 minima are reached at 45cm and 60cm depth, respectively.

Total S (sulfur) shows strong variation with depth at GOF5 and GOF6. The peak at 15cm and 30cm at GOF5 and GOF6, respectively, coincides with the increase in C_{org} at that depth.

At GOF5, Fe bulk profiles display similar trends to S bulk profiles. At GOF6, the peaks in total S are also reflected in total Fe, however not in the same order of magnitude as at GOF5. Furthermore, in the top 10 to 15cm in GOF3 and GOF5, total Fe concentrations are stable but total S concentrations increase with depth

There is a small surface enrichment in total Mn at all three sites, which is also found in the CDB-Mn profiles (Figure 14), indicating the presence of Mn oxides. Overall, the profiles show little variation in Mn with depth, with the exception of a large peak at 25 cm in GOF3. CDB-Mn accounts for almost the entire pool of total-Mn in this peak (Figure 15), indicating that this peak is composed primarily of Mn-oxides. The Mn-oxide enrichment can be coupled to the elevated concentrations at depth of the Mn^{2+} porewater profile (Figure 12).

Note that the accuracy of the data is lower for the peak at GOF3 and at the surface of GOF5 (Figure 15), but this has no consequence for the general signals and does not affect the interpretation of the data.

The Mn-oxide peak at 25cm depth at GOF3 coincides with a peak in CDB-Fe (Figure 14). At GOF5 and GOF6, similar peaks in CDB-Fe are observed at 10cm and 30cm depth, respectively. The similarity of these CDB-P peaks between all the cores suggests simultaneous deposition. At GOF5 and GOF6 these Fe-oxide maxima coincide with the mid-depth peaks in C_{org} . Overall, the CDB-Fe profiles show an decreasing trend from the surface downwards at all sites.

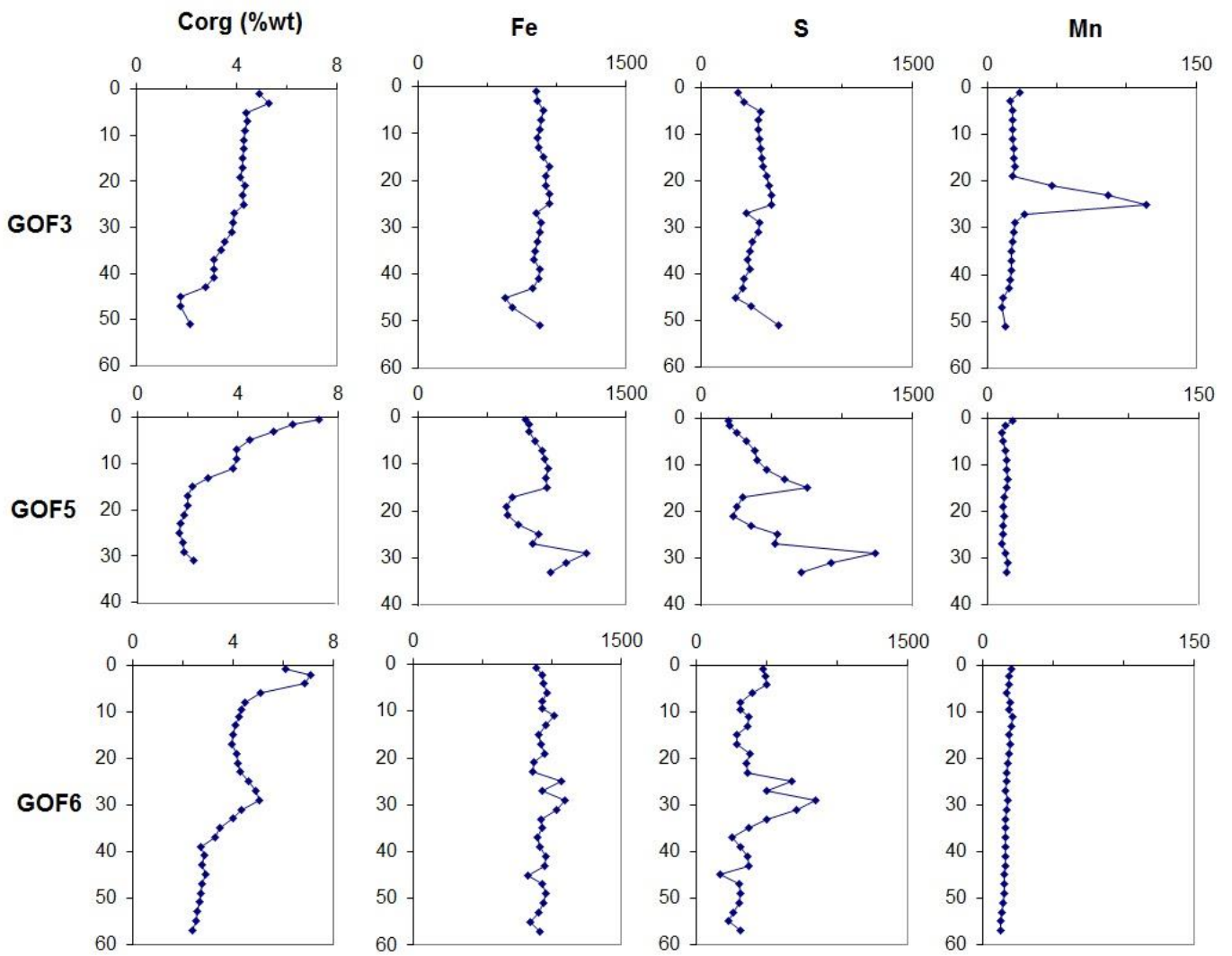


Figure 13. Sediment profiles of organic carbon (%wt) and total Fe, S and -Mn (in $\mu\text{mol/gr}$) for GOF3, GOF5 and GOF6.

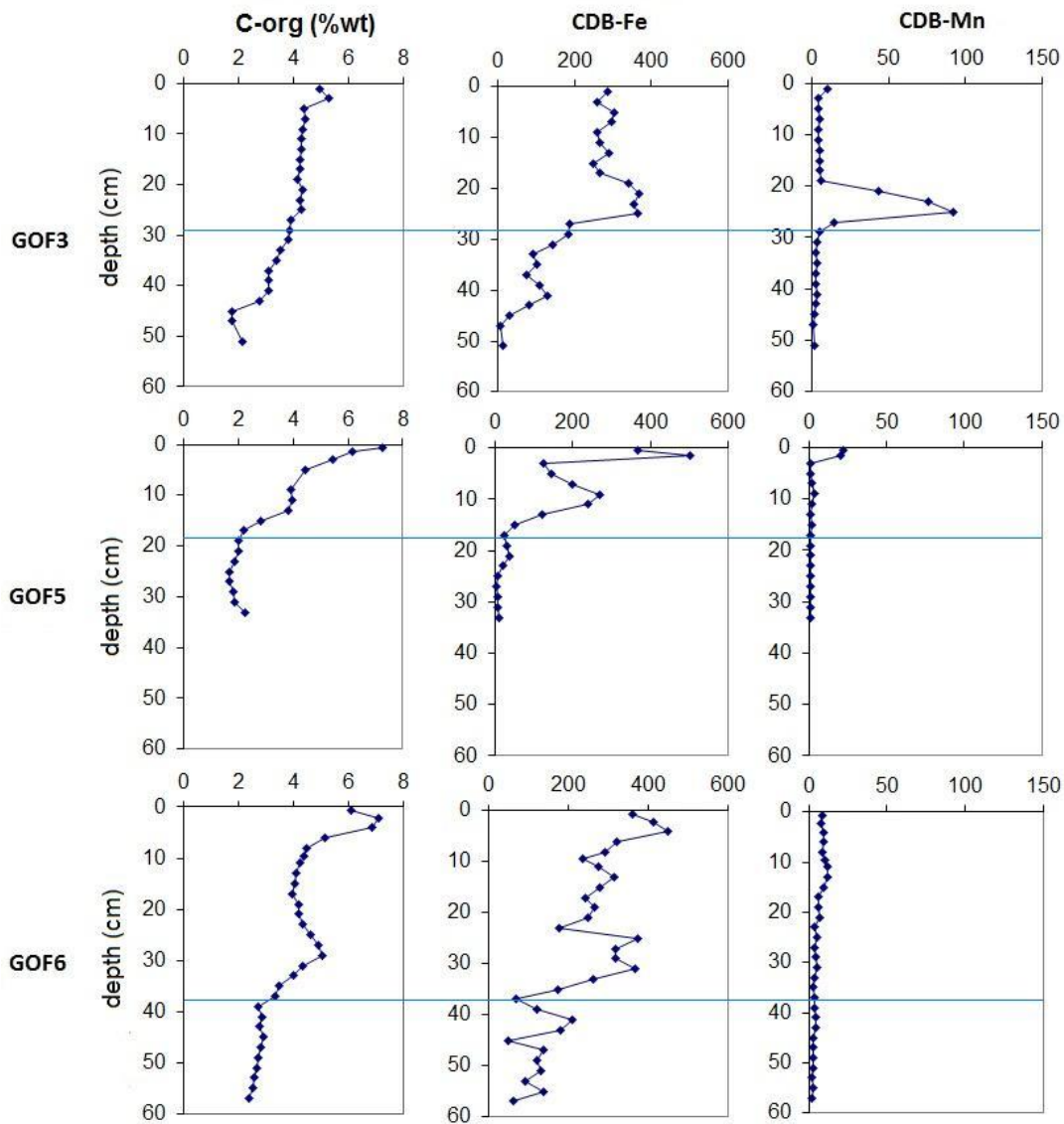


Figure 14. Sedimentary C_{org} (%wt), oxide-Fe and oxide-Mn (ppm) for GOF3, GOF5 and GOF6. Oxide-Fe and oxide-Mn extracted with CDB analysis.

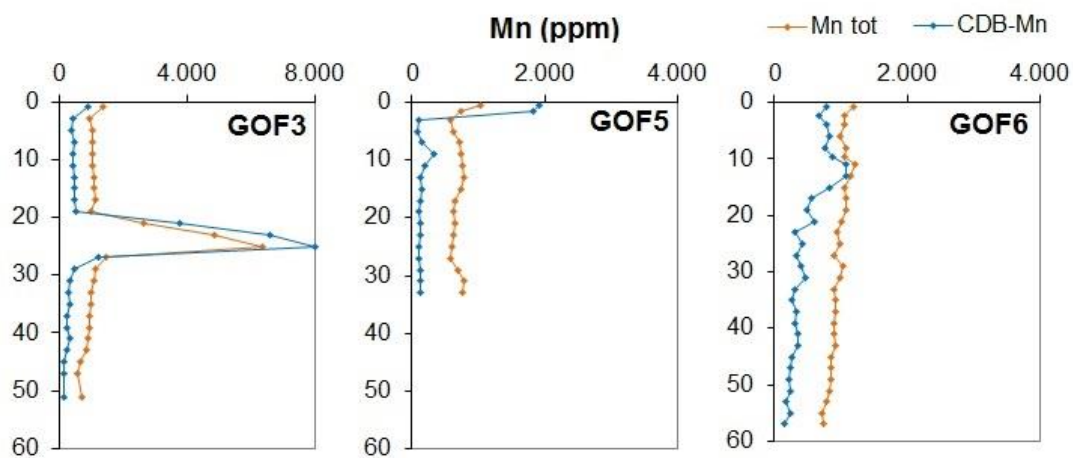


Figure 15. CDB-Mn and Mn total (ppm) for GOF3, GOF5 and GOF6. Note the different scale at GOF3.

4.4 P-species

Fe-P is the dominant phase in which phosphorus is found in the surface sediment (Figure 16). All sites are enriched in Fe-P in the top 5cm, while below this depth concentrations decrease and stay constant with depth. Fe-P concentrations are highest at the surface at GOF5 (100-120 $\mu\text{mol/g}$) and are lowest at depth at constant values of $\sim 4 \mu\text{mol/g}$. At GOF3 and GOF6, Fe-P concentrations generally stay around 10 $\mu\text{mol/g}$ to the base of the core.

Organic P concentrations range between 10 and 15 $\mu\text{mol/g}$ in the surface sediment, and show a decrease with depth to concentrations between 5-8 $\mu\text{mol/g}$. The fluctuations observed in the C_{org} profile (Figure 13) are also present in the organic-P profiles of GOF5 and GOF6 in organic-P. GOF3 shows some variation in organic-P at the bottom of the profile, but the general decrease with depth corresponds with the C_{org} profile.

Acetate P and detrital P are low (10 and 5 $\mu\text{mol/g}$, respectively) and are relatively constant with depth, suggesting there is no in-situ formation. Exchangeable-P concentrations were around 1-2 $\mu\text{mol/g}$ in the surface sediments and dropped to almost zero background values. Since these values are negligible they were not displayed in the results.

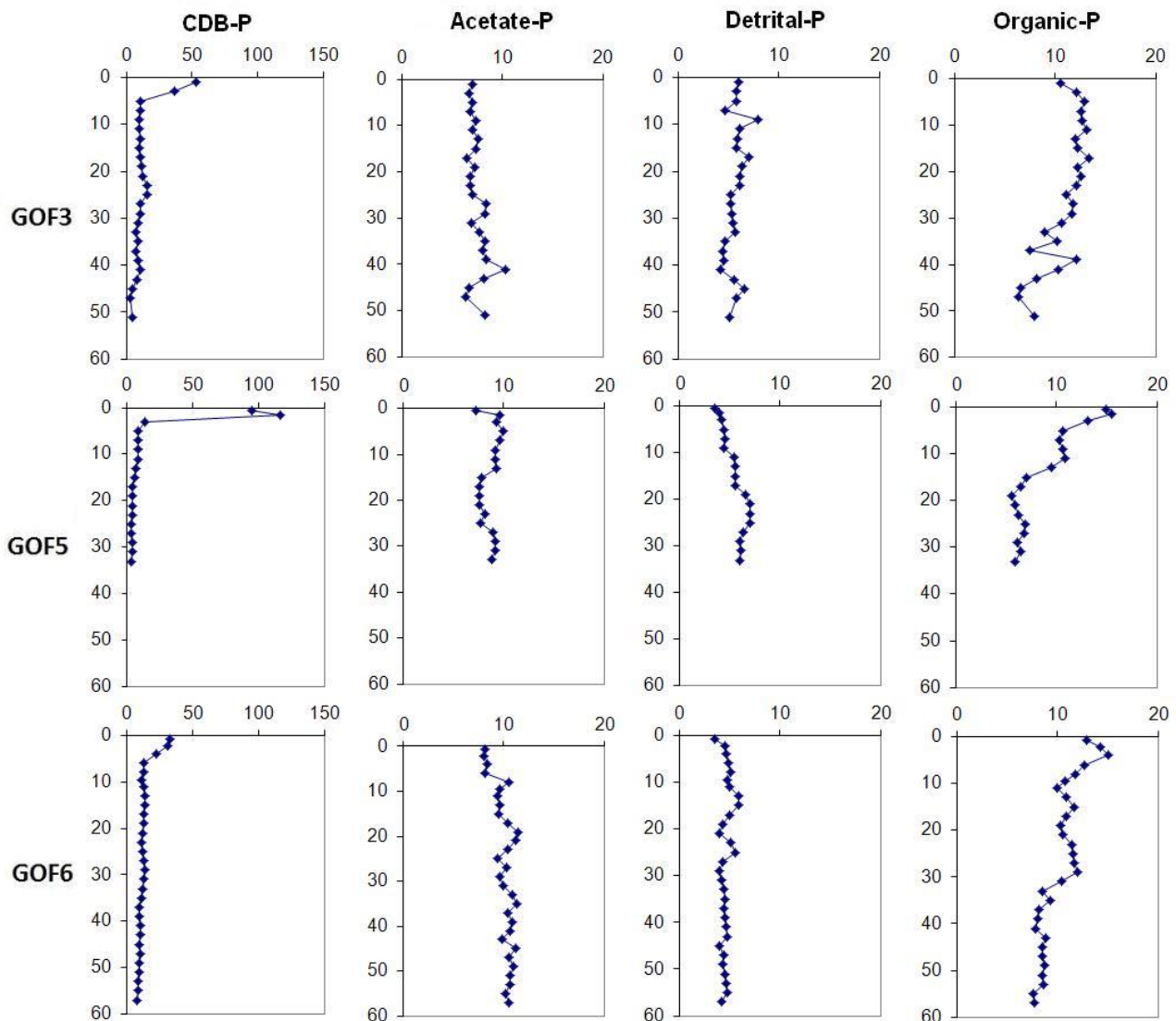


Figure 16. Sediment phosphorus speciation (in $\mu\text{mol/gram}$) for GOF3, GOF5 and GOF6 (according to extraction method described in Ruttenberg, 1992).

5. Discussion

5.1 Oxygen variability in the GOF and Baltic Proper

Major inflows bring saline and oxygen rich water into the Baltic Sea, and are the driving force in long-term and large scale water column processes, which in turn is important for the interpretation of sedimentary signals. During the stagnation period from 1970-1993 the total hypoxic area in the Baltic Sea decreased and after the major inflow of 1993, this area increased again until the second inflow in 2003 (Jilbert et al., 2011).

When comparing the response of bottom water oxygen to stagnation period (1970-1993) and major inflows (1993 and 2003) between the Baltic Proper stations (Figure 11) and the GOF (Figure 10), there are some differences. The Gotland basin sites have a depth range of 175-446m, which is far below the halocline at a depth of ~70m (Meier, 2007; Jilbert et al., 2011). However, not all stations are equally anoxic, and there is no clear relationship between the depth of the station and the

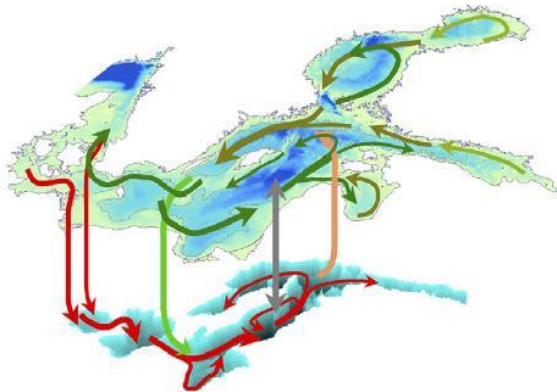


Figure 17. Schematic view of the large-scale circulation (red =bottom, green= surface) in the Baltic Sea. Light green and beige arrows show entrainment, grey arrow is diffusion. (Elken and Matthäus, 2008).

intensity of the anoxia. The response to the major inflows in 1993 and 2003 is clear: there is an increase in bottom water oxygen levels at all four stations, although this response is delayed by approximately one year at BY15.

The response to the stagnation period from 1970-1993 differs between the deep sites. In the Eastern Gotland basin (BY15 and F80) bottom water oxygen concentration decrease during the stagnation, while at F80, after an initial decrease, oxygen levels stabilize. In the Northern Gotland basin, bottom water oxygen levels remain stable during the inflow, despite minor fluctuations. Overall, the stabilizing oxygen levels at BY31, BY29 and F80 indicate that the water masses in these locations were less stagnant than at BY15. Hence, minor inflows were potentially able to reach these sites and create a balance between oxygen supply and further depletion. The quick response of oxygen concentrations to the major inflow of 1993 confirms the idea that inflows have a free flow pathway to these sites.

Site BY15 however, displays an almost uninterrupted decrease in oxygen values during the stagnation period and the response to the inflows is delayed. This raises the possibility that a different mechanism operates here, which prohibits minor inflows to reach this site and delays the effect of major inflows. An explanation could be found in the flow path of the Baltic conveyor belt (Figure 17). This circulation pattern shows incoming water to flow along the Eastern edge of the Gotland basin in an anticlockwise motion around the edges of the deepest part of the basin, in which site BY15 is situated (Meier, 2007). This circular motion probably prevents the inflowing water from reaching the deepest part of the basin directly, thereby delaying the increase in oxygen at site BY15.

In contrast to the Baltic Proper stations, the GOF does not show an increase in bottom water oxygen in response to every major inflow event. Rather, the increasing bottom water oxygen values during the stagnation period (1970-1993) and the decrease in bottom water oxygen values in the period after the inflow (1993-2003) (Figure 10) corresponds well to the expansion and contraction of the hypoxic area as described by Jilbert et al. (2011).

The 1993 inflow is followed by a decrease in bottom water oxygen values, while the 2003 inflow is followed by an increase (Figure 10). The stagnation period prior to 1993 had caused the halocline to be broken down in the GOF, as shown from the salinity data (Figure 10). The 1993 inflow that followed the stagnation period re-established the halocline which caused the oxygen levels to decrease during the following years. The inflow of 2003 shows an opposite response in bottom water oxygen; this time the water column is already stratified and bottom water oxygen levels are raised. This opposite response in bottom water oxygen levels show that the effect of the inflow on bottom water oxygen levels in the GOF is controlled by the depth and strength of the halocline. The timing of the inflows only forces the timing of the changes in the long-term oxygen trend.

Thus, water column processes that operate in the GOF are different from the deepest sites in the Baltic Proper. The effect of an inflow in the Baltic Proper is always to increase oxygen levels, whereas at the GOF, a major inflow brings oxygen rich waters but the effect is controlled by the intensity of the halocline prior to the inflow. In the GOF during Baltic-wide stagnation periods, stratification can be completely eroded, leading to a complete ventilation of the water column. Although this process is slow, its impact on bottom water oxygen is significant.

Figure 10 illustrates that the study sites in the GOF are also subject to large seasonal variations in bottom water oxygen. The seasonally dependent organic matter flux leads to a yearly cycle of contraction and expansion of the hypoxic area (Conley et al., 2002). This is an important process in the GOF, causing bottom water conditions to be seasonally hypoxic depending on the point in time on the long-term trend. Hence, the combination of biological factors from eutrophication and physical factors from inflows cause the sediments in the GOF to be subjected to non-steady state conditions on a monthly, yearly and decadal basis.

It should be noted that the cores used in this study were collected during early spring (May 2009), which is at the onset of the decrease in oxygen levels as a result of deposition of the spring bloom (Reed et al., 2011). In Figure 18 the average bottom water oxygen values are plotted for each month, and here is shown that bottom water oxygen has not yet reached its minimum during May. The Fe-P

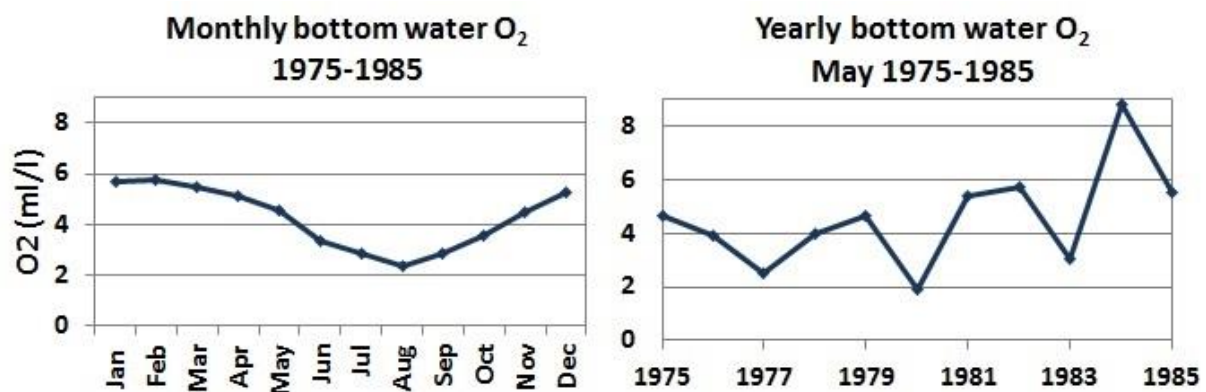


Figure 18. Left: seasonal bottom water O₂ variation in GOF at 70m depth, averaged over years 1975-1985. Note that these are not absolute values, and the trend can shift up or down depending on the point in time in the large-scale trend. Right: May bottom water oxygen values from 1975-1985.

peaks found in the surface of the cores are a seasonal signal, and should not be seen as absolute values since dissolution of Fe-oxhydroxides (and release of associated P) may be expected in the months following (Reed et al., 2011).

5.2 Sediment records of redox history

Fluctuations in C_{org} content in the sediment indicate non-steady state conditions and can be caused either by a change in redox conditions or organic matter flux to the sediments, or a combination of both. Furthermore, C_{org} in the sediment is influenced by the ongoing degradation of organic matter after deposition.

Molybdenum has been shown to be a reliable proxy for hypoxia in the Baltic Sea due to the absence of depletion during hypoxic events, despite the semi-enclosed character of the Baltic Sea (Jilbert and Slomp, 2013b). Therefore Mo can be used to help distinguish the productivity signal from the redox signal in the C_{org} profiles (Figure 19).

The modern hypoxic event is characterized by increased productivity and a consequent elevated flux of organic matter to the sediments (Gustafsson et al., 2012). This is reflected in a long-term gradient of decreasing C_{org} concentrations with depth at all sites (Figure 13). For example at GOF6, the baseline C_{org}

concentration increases from 1950-2000, with a peak of higher concentrations superimposed at ~1970 (Figure 18). In contrast, the Mo/Al profile for the same interval shows the peak but not the increasing baseline from 1940 until present day. This suggests that the increasing baseline in C_{org} is related to rising productivity and thus carbon flux to the sediments (independent of bottom water oxygen concentrations), while the peak in both Mo/Al and C_{org} around 1970 is related to low oxygen conditions at this time. The water column data support this interpretation (Figure 10). The effect of degradation on C_{org} profiles is usually limited to the top few centimetres of the core, and therefore cannot explain the baseline increase that was found throughout the core. Modeling work by Dan Reed (unpublished results) shows that to simulate similar baseline increase in cores from elsewhere in the Baltic, an increase through time in the flux of C_{org} has to be assumed.

Although the Mo/Al and C_{org} signals are also captured at GOF5, the lower Mo/Al concentrations suggests that the intensity of reducing conditions were less extreme than at GOF6, despite the similar C_{org} concentrations. Moreover, the lack of variability in the C_{org} profile at GOF 3 (Figure 13) suggests that oxygen concentrations have not significantly changed at this site, despite the general increase in C_{org} input. So despite the upward shift of the redoxcline from 1950 to 1970, GOF3 has remained above the redoxcline and bottom water concentrations never became hypoxic. The development of the redox history in the GOF combined from the water column data (Figure 10) and sedimentary redox indicators (Figure 19) is summarized in Figure 20.

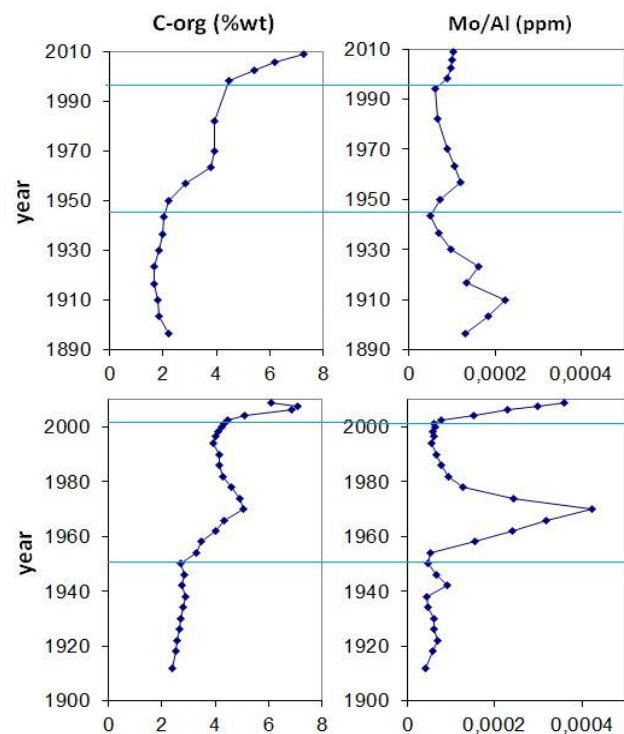


Figure 19. C_{org} %wt and Mo/Al at GOF5 (upper) and GOF6 (lower) against time. Mo is normalized to Al to separate the redox signal from variations in sedimentation.

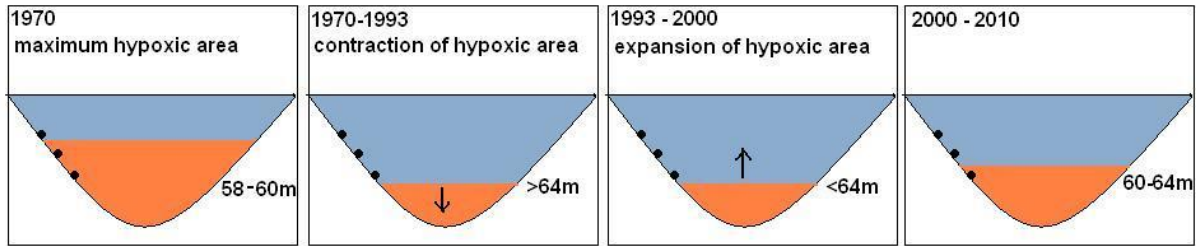


Figure 20. Summary of redox history in the GOF, with cores GOF3, GOF5 and GOF6 indicated on slope. Red area represents the area below the halocline.

5.3 The impact of redox conditions on sedimentary geochemical cycles

Changes in redox conditions through time and space impact the cycles of redox sensitive elements, such as iron, sulfur and manganese. In normal (non-euxinic) terrigenous marine sediments, organic matter is the limiting factor for pyrite formation (Berner, 1984). Since the GOF is a coastal marine sediment with generally oxic bottom waters, this is probably true for the GOF.

At GOF3, there is minor variation in the profiles of C_{org} , Fe and S, despite a variable flux of Fe-oxides through time (Figure 13). This supports the theory that at GOF3 there is C limitation with respect to pyrite formation. Conversely, non-steady state conditions at GOF5 and GOF6 during the hypoxic period around 1970 provided increased availability of both C_{org} and Fe-oxides. This enabled the formation of pyrite, reflected in the Fe and S peaks at middepth at GOF5 and GOF6 (Figure 13).

Fluctuation in the total iron supply to sediments is caused by the shuttling of reactive iron from the shelf into basin (Lyons and Severmann, 2006). During periods of increased hypoxia, reactive iron from the oxic/suboxic shelf is remobilized when a shallowing halocline comes into contact with sediments rich in Fe oxides which consequently dissolve. The reactive iron that is released either reprecipitates as oxides at shallower depths or precipitates as pyrite at greater depth where H_2S concentrations are higher and oxygen is depleted. According to this theory, hypoxia generally leads to a decrease in oxide formation or even a loss through shuttling in sediments within the halocline (Lyons and Severmann, 2006). Therefore it is perhaps unexpected that we find Fe-oxide enrichments during hypoxic conditions at all sites (Figure 14). However, water circulation patterns may influence the distribution of dissolved reactive iron and deposition of Fe oxides in marine basins. Circulation in the GOF is anticlockwise (Figure 6). This may explain the enrichments of Fe oxides close to the redoxcline on the Northern slope of the GOF during periods of increased hypoxia. Fe dissolved into the inflowing water from the Southern slope, which experiences more severe gradients in salinity and hence oxygen (Figure 7B), may be redeposited on the Northern slope which remains relatively oxic at all times.

In (Figure 21) Fe versus S is plotted. The main observation is the strong linear Fe:S correlation at GOF6 to a molar ratio of 1:2, providing evidence that at this site almost all reactive Fe is present in the sediment as pyrite. For GOF3, there is also a clear correlation matching a molar ratio of 1:1 starting at elevated S concentrations. The ratio 1:1 indicates the presence of iron monosulfide (FeS), suggesting that not all iron sulfides are transformed into pyrite. This difference in composition reflects the less hypoxic conditions at GOF3 compared to GOF6. Explanations for the elevated S concentrations at GOF3 remain speculative without specification of sulfur species. Furthermore, there is some scatter around the trendline in Figure 21, especially at GOF5 but also at GOF3. The points below the line show a depletion of sulfate relative to iron, which indicates the presence of iron oxides since this is the other main phase in which reactive iron can be found. The low correlation

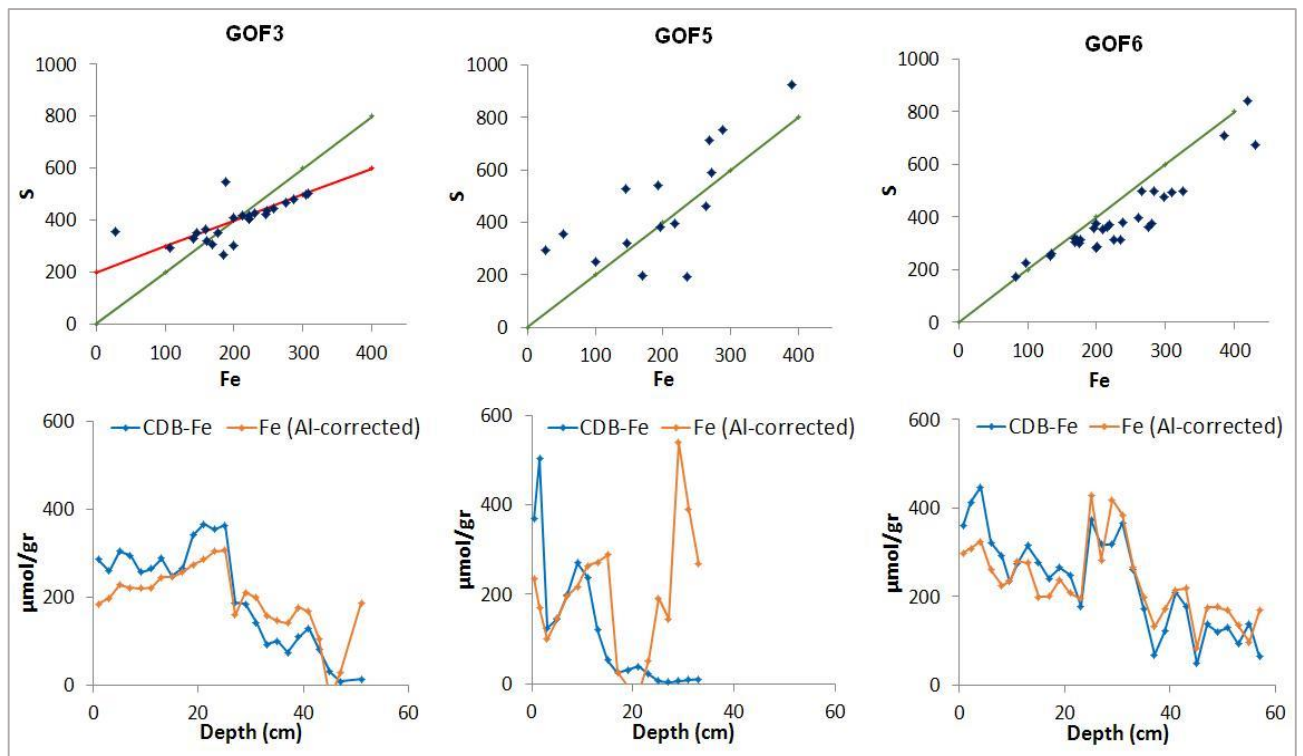


Figure 21. Top: plot of Fe (corrected for aluminium) versus S. The green line indicates ratio 1:2, the red line at GOF3 indicates 1:1 ratio with elevated S concentrations. Bottom: Oxide-Fe and Fe corrected ($\mu\text{mol}/\text{gr}$) against depth (cm). Correction for Fe was done using Fe/Al ratio of 0.5 for average shale (Taylor and McLennan, 1985).

between Fe and S at GOF5 indicates a large amount of iron oxides at this site. If all of reactive iron at GOF6 is captured in pyrite, as for a part of reactive iron at GOF3, the close match between the CDB-Fe and Fe total (Figure 21) indicates that these fractions are in fact the same. This means that pyrite was dissolved during CDB extraction. Dissolution is known to occur due to the strong complexing activity of the citrate and, possibly, by instability of the pyrite in the oxidized environment of the surface sediment (Slomp, et al., 1996). Although the CDB-Fe fraction at GOF3 and GOF6 are mainly iron mono-sulfide and pyrites, respectively, it is likely that they were originally deposited as Fe-oxides. Early pyrite forms almost exclusively from iron oxide (Canfield, 1989), so reductive dissolution of these iron oxides after burial enabled the reactive iron to reprecipitate as pyrite.

At the bottom of the core at GOF5 there is a peak in Fe and S which is larger than the peak at middepth (Figure 13). The mechanism by which this largest peak is formed cannot be explained in the same way as the peaks at middepth at GOF5 and GOF6, which correspond to simultaneous increases in C_{org} and Mo and water column redox changes, and therefore appear to be a redox related signal. Since the C_{org} profile doesn't show a significant increase, the largest peak at GOF5 is probably not formed during a period of increased hypoxia.

An explanation for the formation of this peak could be that it is a recent signal, formed after deposition due to a shift in the sulfate methane transition zone (SMTZ). The SMTZ is a boundary layer in the sediment where pore water sulphate and methane concentrations intersect at non detectable concentrations, due to the coupling of anaerobic oxidation of methane through sulfate reduction. This leads to a production of sulfide which can reductively dissolve reactive iron to form Fe-sulfides. Therefore the accumulation of such Fe-sulfides can be indicative for SMT zones. This was also found in the Bothnian Sea, where a distinct maximum in S and Fe was observed at the SMTZ (Slomp et al., 2013).

The elevated Mo concentrations at the bottom of GOF5 support this idea (Figure 19). Mo has been found to show elevated concentrations within the SMTZ, where elevated H₂S concentrations allow Mo to be scavenged by FeS (Peketi et al., 2012). A barium (Ba) front is also known to develop just above the SMTZ (Dickens, 2001). Barium profiles are plotted in Figure 22. There is a small excursion in the Ba concentrations at GOF5 at a depth of 30cm. This excursion could indicate the presence of the SMTZ, but it is very small. The signal could be diminished due to a low productivity- linked Ba flux to the sediment or Ba could be dissolved due to an upward movement of the SMTZ (Peketi et al., 2012). Nonetheless, evidence for the presence of a SMTZ from the Ba profile is weak.

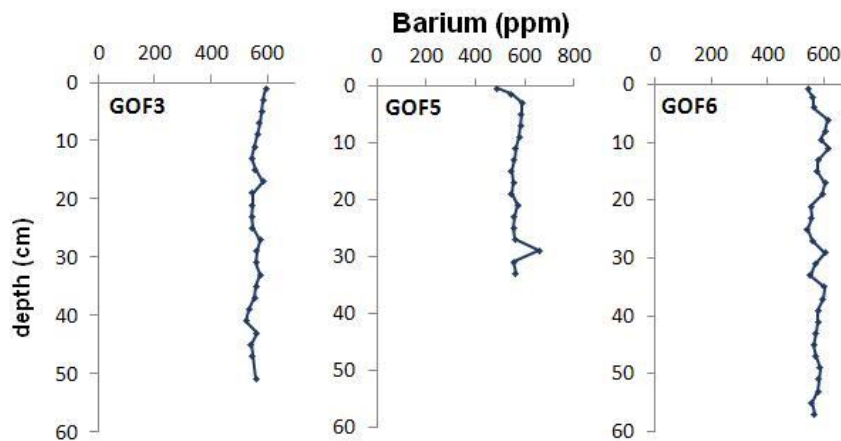


Figure 22. Barium (ppm) against depth for GOF3, GOF5 and GOF6.

A conclusive interpretation that the peak at depth at GOF5 was related to a shift in the SMTZ remains speculative. Evidence from porewater data is inconclusive and poses many new questions (Figure 12). SO₄²⁻ is much more rapidly depleted at GOF3 and GOF6 than at GOF5 (where we see no depletion), indicating a much shallower and more sharply defined SMTZ at the former two sites. However, at GOF3 there is no signal in Fe and S, and at GOF6 we do not see a second peak like at GOF5. At the sites in the Bothnian Sea there is a complete depletion of SO₄²⁻ even below the depth where such peaks are found, at GOF5 we do not see a complete depletion. Furthermore, at none of the sites in the GOF do we find an increase in porewater Fe²⁺ below the SMTZ zone as observed in the Bothnian Sea. Since the Fe-S peak at GOF5 is situated at the bottom of the core and we cannot see what happened at greater depth it remains difficult to explain what caused this peak and the apparent discrepancy between the sites GOF5 and GOF6.

While the direct influence of the shallowing halocline is not recorded at GOF3 in C_{org}, S and Fe, the distinct peak in Mn-oxides (Figure 14) is likely an indirect result of the increasingly reducing conditions at greater water depth. Such enrichment is not found elsewhere in the Baltic Sea, although it is a widespread phenomenon in the Black sea, as described by Reitz et al., 2006. Large Mn-enrichments can be deposited just above the redoxcline during periods of increased anoxia. Sediments overlain by anoxic waters release Mn²⁺, and this leads to a buildup of Mn²⁺ in the anoxic bottom waters (Balzer, 1982; Kristensen et al., 2003). Sediments above the redoxcline, which are overlain by relatively oxic waters, have the capacity to precipitate large amounts of Mn-oxides. This can happen by upward diffusion of Mn²⁺ through the redoxcline or rapid fluctuations of the redoxcline that bring relatively oxic sediments into contact with Mn²⁺ enriched waters from below the redoxcline. This would explain the large amount of Mn-oxides at GOF3. These are not Mn-carbonates, since the carbonate profile shows no excursion at GOF3 (Figure 23).

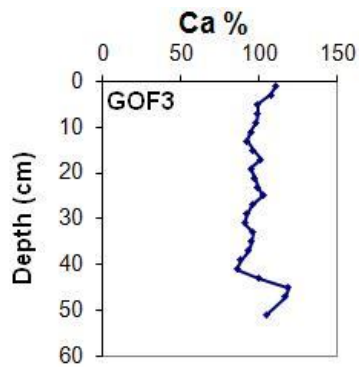


Figure 23. Carbonate profile (%) for GOF3.

Dellwig et al., 2010 provided evidence for a succession of Mn- and Fe- species along a redox gradient: Mn-oxides are typically found above the redoxcline, and Fe-oxides precipitate within or just below the halocline through the reduction of Mn-oxides. Accordingly, we find high concentrations of Mn-oxides at GOF3, confirming the idea that GOF3 was situated above the redoxcline during the interval of expanded hypoxia centered on ~1970. The elevated porewater Mn^{2+} concentrations that were measured at depth at GOF3 (Figure 12) indicate ongoing reduction of the buried Mn-oxides at this site. At GOF5 and GOF6, Mn-oxides may have also precipitated around 1970, since it is also present in the surface layers today. However, the fact that we find no trace of these deposits today means that Mn-oxide precipitation occurred to a lower extent than at GOF3, and in addition the lower oxygen concentration at greater depth would have caused enhanced reduction of Mn oxides by Fe oxides as described by Dellwig et al. (2010).

5.4 Spatial variability in redox conditions and organic matter input along the GOF transect

5.4a Water-depth gradient

Redox conditions vary not only through time but also with increasing water depth. Porewater data confirm the increasingly reducing conditions that we expected to find with increasing depth. The signal in the oxygen profiles complements with the sulfate profiles. Oxygen seems to be present in the top surface layer at all sites, confirmed by the bottom water oxygen data, despite the deviating profile at GOF6 (Figure 12). Sulfate reduction starts at greater depth at GOF3 and GOF5 than at GOF6, where concentrations decrease from the top. This means at GOF6, SO_4^{2-} is the main reducer from the top of the sediment. Also the zero Fe^{2+} surface concentrations at GOF6 suggests all porewater Fe^{2+} is quickly scavenged by H_2S to precipitate as iron sulfate or pyrite, whereas at GOF3 and GOF5 small concentrations of porewater Fe^{2+} show a build up near the surface.

The $C_{\text{org}}/P_{\text{org}}$ ratio is an important redox indicator due to the favourable release of P from organic matter under anoxic conditions (Algeo and Ingall., 2007). The effect of the redox gradient on the cores is clearly reflected by this redox proxy and also Mo (Figure 24); both show an increase with depth indicating more reducing conditions.

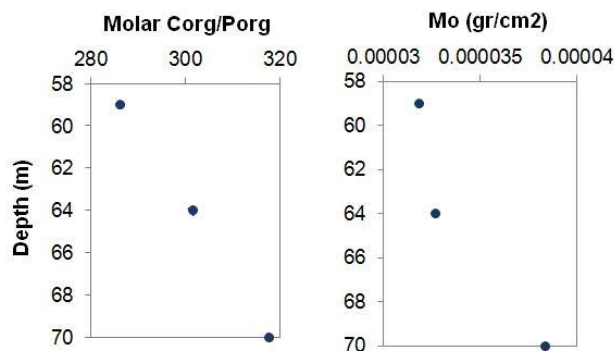


Figure 24. Left: Sedimentary $C_{\text{org}}/P_{\text{org}}$ ratio of GOF3, GOF5 and GOF6 against water depth. Values are averages of the $C_{\text{org}}/P_{\text{org}}$ ratios at each site over the top 30cm of the cores. Right: Cumulative Mo for GOF3, GOF5 and GOF6 over the top 15cm of the cores.

Also the oxygen gradient has an effect on the biological activity. Biological activity was found at GOF3 and GOF5, but not at GOF6 (Josefson et al, 2012). The irregularity at 18cm depth in the porewater data at GOF3 (Figure 12) is likely the result of a burrow. It should be kept in mind that mixing of the sediment by organisms occurs at GOF3 and GOF5, and this may have influenced the signals we see in the chemical profiles. However, during periods of increased hypoxia, GOF5 became more hypoxic and at these times biological activity probably decreased. Since GOF3 has always been situated above the halocline, biological activity at this site was probably not affected.

5.4b Independent of oxygen

The flux of organic and inorganic material to the sediment causes significant differences between the sites, independent of bottom water oxygen concentrations. However, the organic matter flux to the sediment controls the sedimentary oxygen consumption and this interaction plays an important role in the elemental cycles of iron, sulfate, manganese and phosphate.

As we expected, the high C_{org} concentrations (6-7%wt) in the surface sediment (Figure 13) confirm that the GOF is a high productivity area. And although the surface C_{org} concentrations are the same at all three sites (meaning the ratio of carbon input to other sediment components is similar between the sites), the total amount of C_{org} accumulated over the top 30 cm is lower at GOF5 (Figure 25). Since oxygen concentrations at the sediment surface are in the same order of magnitude along the

GOF transect, this signal is independent of bottom water oxygen concentrations. The lower total C_{org} content can therefore only be caused by smaller OM flux to the sediment. The deviating porewater NH_4^+ and SO_4^{2-} flux rates at GOF5 (Figure 25) support this idea by showing lower remineralization rates at GOF5.

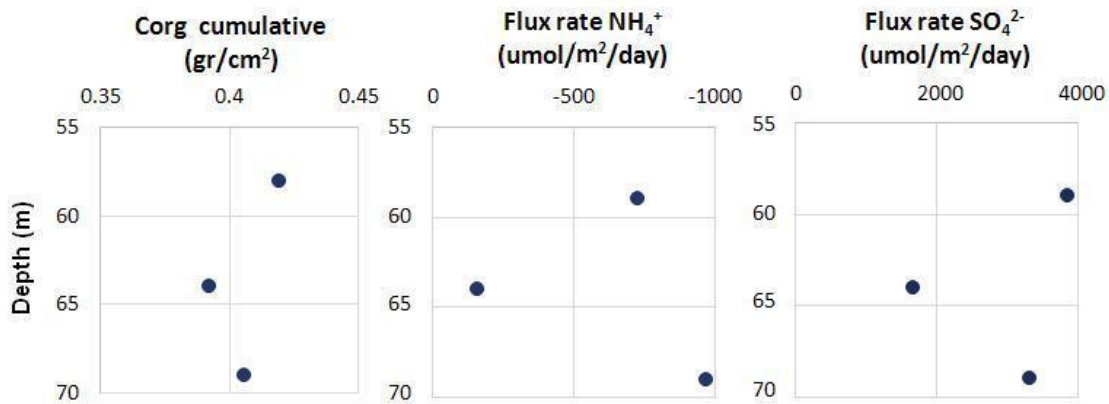


Figure 25. Cumulative C_{org} (gr/cm²) over the top 30cm of the sediment. NH_4^+ flux rate and SO_4^{2-} flux rate at GOF3, GOF5 and GOF6 calculated using Fick's law: $F = -\frac{\phi D}{\theta^2} \frac{\delta C}{\delta z}$. Where F = flux in $\mu\text{mol}/\text{m}^2/\text{day}$, D =ion specific diffusion coefficient from Boudreau (1997), $\delta C/\delta z$ = concentration gradient, from uppermost porewater sample to the bottom-water sample (for NH_4^+) and the steepest inter-sample gradient in the porewater decline (for SO_4^{2-}), ϕ = porosity and θ = tortuosity as defined by Boudreau (1997): $\theta^2 = 1 - \ln(\phi^2)$.

For GOF5, the lower remineralization rate causes a lower sedimentary oxygen demand, which makes the surface sediments at this site relatively oxic compared to the other two sites. The relative high oxygen availability at GOF5 favours the formation of large amounts of iron oxides. Fe-P concentrations at GOF5 are more than double compared to GOF3 and GOF6 (Figure 16). Interesting to note however, is that an organic matter based redox proxy like C_{org}/P_{org} proves to be independent of this secondary oxygen effect (Figure 24).

Characteristic for sediments with an intact layer of iron oxyhydroxides at the sediment-water interface are low porewater HPO_4^{2-} values in the surface layer (Jilbert et al., 2011; Slomp et al., 1996; Slomp et al., 1998), since iron oxides trap the HPO_4^{2-} from the porewater. Jilbert et al., 2011 (Figure 3a therein) have measured anomalously high NH_4^+/HPO_4^{2-} flux ratio's at GOF5, ($NH_4^+/HPO_4^{2-} = 83$), whereas for GOF3 and GOF6 these values approach zero. This is confirmed by the absence of HPO_4^{2-} in the top 5cm at GOF5 (Figure 12). Figure 14 shows Fe-oxide concentrations, and the same results are also found here, e.g. highest at GOF5 and roughly double of the concentration at GOF3. The ratio of Fe:P ratio in Fe-oxides at the GOF sites is ~1:6. This is lower than the ratio determined by Slomp et al., 1996, who found the ratio of P bound to poorly crystalline iron oxides has been determined to be $\pm 10:1P$ for coastal and shelf sediments. Furthermore, Mn-oxides in the surface sediment are also highest at GOF5, and double of the concentration in the surface sediment of GOF3 (Figure 14). Porewater Mn^{2+} at GOF5 is most depleted in the surface sediment, probably due to the higher scavenging from Mn-oxides. The peak Mn^{2+} concentrations in the surface at the other sites could be enhanced by the higher sedimentation rates which prevents significant Mn^{2+} loss to the water column (Shimmield and Pedersen, 1990).

5.5 Phosphorus

Overall, concentrations of organic P, Acetate-P and background values of CDB-P are in the same order of magnitude at the GOF sites. The linear profiles of Acetate-P provide no evidence for sink-switching from P-org or Fe-bound P to acetate P (Ruttenberg and Berner, 1993). It can be concluded that Acetate-P in the GOF is unreactive and plays no role in the phosphorus budgets with respect to the feedback mechanisms on eutrophication. This is in line with what has also been found in 5 out of 6 locations in the Southern and central Baltic Sea (Mort et al., 2010) and in the Bothnian Sea (Slomp et al., 2013).

Organic P concentrations are relatively high, and form an important burial phase in the GOF, as in the rest of the Baltic (Mort et al., 2010). The P_{org} burial is higher during the hypoxic event around 1970 (at 10cm GOF5, 30cm GOF6), and also show a general increase over time (Figure 16). The organic P profiles are similar to those of C_{org} (Figure 13). This coupling is caused by the fact that organic matter is the host phase for P-org. Consequently the C_{org}/P_{org} ratio with sediment depth time resembles the C_{org} profiles, showing an increasing trend towards the surface (Figure 26). There is scatter in the C_{org}/P_{org} profiles, and the peaks at middepth in C_{org} are less clearly visible in the C_{org}/P_{org} profiles.

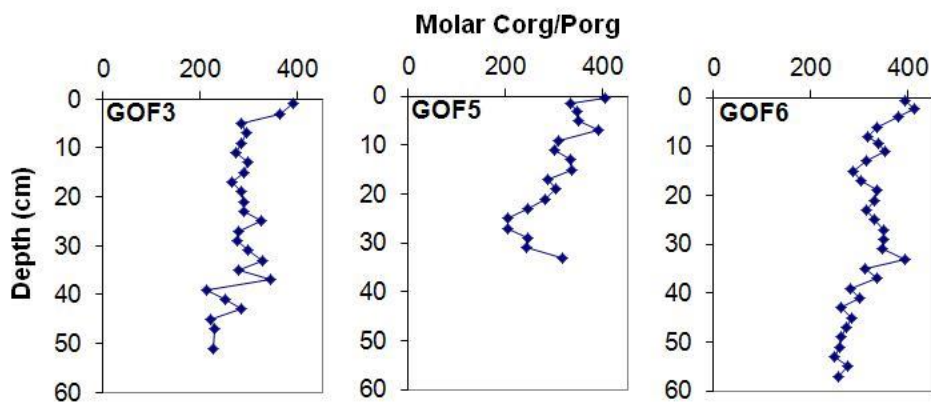


Figure 26. Sedimentary C_{org}/P_{org} ratio (mole/mole) for GOF3, GOF5 and GOF6 against sediment depth.

Fe-P consists of both Fe oxyhydroxide associated P (Ruttenberg, 1992) and Fe(II) phosphates (Nembrini et al., 1983). In the surface layer, this Fe-P consists of mainly iron oxyhydroxides (Figure 16). This is not a permanent sink, since much of this fraction will be returned to the water column (note that sampling was done in May) as oxygen levels drop in the fall due to remineralization of the organic matter from the spring bloom (Reed et al., 2011). Despite this, we find small fraction of Fe-P at depth which likely consists of Fe (II) phosphates (mainly vivianite). With background values of $\sim 8 \mu\text{mol}/\text{gr}$, this can be considered significant as a long-term sink for P in the GOF (Figure 27).

Jilbert and Slomp (2013a) also found Fe (II) phosphates both in the deep basin (F80) with background values of $10 \mu\text{mol}/\text{gr}$ and at site LF1 (67m) where background values were considerably lower, around $3\text{-}4 \mu\text{mol}/\text{gr}$.

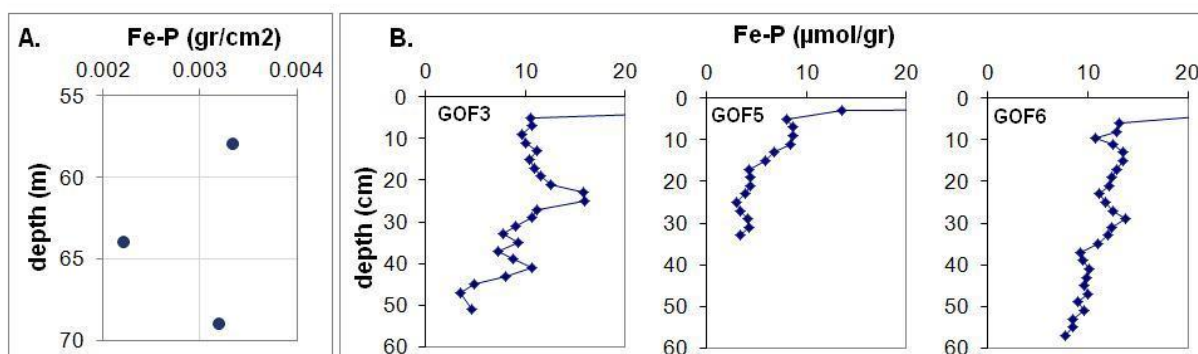


Figure 27. a. Cumulative Fe-P (gr/cm²) over depth interval 5-33cm for GOF3, GOf5 and GOF6. b. Fe-P (μmol/gr), similar to Figure 7, but on adjusted axis for the background.

These results indicate that 1.) substantial amounts of Fe (II) phosphate are formed at sites situated above and within the redoxcline (GOF3-5-6), as well as in the deepest and most oxygen-depleted basins (Jilbert and Slomp, 2013a), 2.) the Fe (II) phosphates at the GOF sites are formed within the shallow sediments in the absence of porewater iron, unlike the processes described by Slomp et al. (2013) for the Bothnian Sea, in which Fe (II) phosphates form below the Sulfate Methane Transition (SMT). Vivianite, a common Fe (II) phosphate, is typically known to precipitate below the SMT where porewaters are saturated with Fe²⁺ and PO₄²⁻ (Schulz et al., 1994, März et al., 2008).

Although we did not measure porewater methane or sulfide, the declining sulfate concentrations in the GOF cores suggest that the SMT is located in the upper sediments, and hence that the Fe (II) phosphate formation we observe takes place in the SMT, as found by Jilbert and Slomp (2013a). Milucka et al. (2012) provide evidence for a potential vivianite formation mechanism within the SMT; they observed intracellular precipitates of Fe(II) phosphate within cells of *Desulfosarcina* (DSS) bacteria. These DSS bacteria take up the HS₂⁻ produced by sulfate reducing methanotrophic ANME-2 bacteria. Together they control the anaerobic oxidation of methane in the sediment, and are thus abundant within SMT environments. The abundance of organic matter determines the amount of methanogenesis at depth, and consequently the CH₄ concentrations from which these bacteria live. This way reducing conditions caused by hypoxia and a high sedimentary organic matter content create conditions favorable for ANME and DSS bacteria to live. High abundances of these bacteria may allow for high Fe (II) phosphates to be found in the sediment. This could explain why similar background concentrations of vivianite were found at F80 and in the GOF, and much lower concentrations at LF1.

The influence of C_{org} content is also reflected in the differences between GOF3, GOF5 and GOF6. Fe oxide concentrations are highest in the surface at GOF5, nonetheless cumulative Fe-P is lowest at GOF5 (Figure 27a). The lower cumulative C_{org} and lower SO₄²⁻ flux rates at this site (Figure 25) indicate that lower rates of remineralization at this site are limiting Fe-P authigenesis by DSS bacteria. Also, when looking in closer detail to the distribution of Fe-P at depth (Figure 27), there is some fluctuation. The peaks at 23cm, 10cm and 30cm for GOF3, GOF5 and GOF6, respectively coincide with the increase in Fe oxides and C_{org} (Figure 14) during the more severely hypoxic interval around 1970. Again, increased C_{org} concentrations appear to stimulate the conversion of Fe oxides to Fe (II) phosphates. So here we find evidence that hypoxia increases P burial in the form of vivianite in the GOF.

6. Conclusions

In this study we analysed the biogeochemistry of three sediment cores that were taken along a transect on the Northern slope of the GOF, a highly eutrophied subbasin in the Baltic Sea. We compared the results with bottom water oxygen data since the mid 1950's, both in the GOF and more broadly in the Baltic Proper, to determine how redox changes in the water column affected sedimentary processes and ultimately influenced phosphorus burial.

In the deep basins of the Baltic Proper, anoxia has been persistent in recent decades, only being interrupted for short periods in response to major inflows from the North Sea. This causes sediments in the deep basin to be closed off from oxygen exchange with shallow water. In contrast, the GOF is a shallow basin with short water residence time and rapid internal dynamics. Consequently the GOF sites are subject to decadal and yearly changes caused by inflows but also to seasonal variations in redox conditions. Due to the location of the studied sites near the redoxcline, bottom water and sediment conditions at these sites respond to the contraction and expansion of the hypoxic area in the entire Baltic Sea. GOF5 and GOF6 experienced periods of hypoxia but never became anoxic. Conditions at GOF3 remained oxic, which allowed large amounts of Mn-Oxides to precipitate and be buried before reduction at this site. This is commonly found in the Black Sea (Reitz et al., 2006), but never before seen in the Baltic Sea.

High C_{org} concentrations in the surface sediments (5-7%wt) confirm that the GOF is a high productivity area at present. A general increasing trend in C_{org} concentrations towards the sediment surface over the entire length of the cores reflects the ongoing increase in productivity over the past century. Non-steady state signals superimposed onto this trend in redox sensitive elements like C_{org} , Mo, reactive Fe and S reflect redox changes in the water column. The excursions in C_{org} around 1970 are the result of increased hypoxia at this time, related to the expanded hypoxic area throughout the Baltic. This is confirmed by coinciding elevated Mo concentrations. At this time, there were also elevated fluxes of iron oxides to the sediment at all sites. These iron oxides were reduced after deposition and the reactive iron reprecipitated as pyrite or iron monosulfide. Especially GOF6 shows a strong pyrite correlation. The mechanism behind the formation of the large coinciding S and Fe peaks at the bottom of GOF5 could be a diagenetic signal caused by a shift in the SMTZ. Still, evidence to support this is inconclusive.

Although results overall show increasingly reducing conditions with increasing water depth, the most significant differences between the sites are forced by the total amount of organic matter that is received at the sediment surface. The lowest total C_{org} content at GOF5 leads to lower remineralization rates at this site, causing a relatively lower sedimentary oxygen demand at this site compared to GOF3 and GOF6.

P_{org} forms an important burial sink, and concentrations have increased since the beginning of the 1900's. Furthermore, high background Fe (II) phosphate concentrations were found in GOF sediments, which support the theory of Jilbert and Slomp (2013a) that 1.) this is an important long-term burial phase for phosphorus, and 2.) such minerals can form within shallow anoxic sediments despite the absence of free porewater iron. However, concentrations in GOF were similar to what was found in the deep basins of the Baltic Proper, thereby contradicting their theory that Fe(II) phosphate authigenesis is forced only by shelf-to-basin shuttling of Fe- and Mn oxides. Our results show that Fe (II) phosphate formation in the GOF is elevated during periods of increased hypoxia and total cumulative background concentrations are highest at sites with highest total C_{org} content. This indicates that Fe (II) phosphate authigenesis is connected to the anaerobic degradation of organic matter, potentially by the production of sulphide and the subsequent rapid reduction of phosphate-loaded iron oxides.

According to our findings Fe-P burial on the Northern slope of the GOF is of the same order of magnitude as what was found in the permanently anoxic sites in the Baltic Proper. The Northern slope of the GOF can be quantified as oxic and seasonally hypoxic situated in high productivity areas (5-7% wt C_{org}) and comprises an area 205000 km³. Budget calculations now underestimate Fe (II) phosphate as a long-term burial sink in this area, and should be reconsidered. Furthermore, there are probably other areas similar to the Northern slope of the GOF which are underestimated in budget calculations, like the Southern slope of the GOF and shallow parts of the Baltic Sea. More research should be done here to further improve budget calculations.

Acknowledgements

Foremost, I would like to thank Tom Jilbert for his supervision, his patience and flexible approach with which he helped me to finish this thesis. Also I would like to thank Caroline Slomp, I am grateful for the time and chance that was given me to start and finish this project.

I thank both of you for the many discussions and the useful comments.

Furthermore I would especially like to express my gratitude to Bo Gustafsson for his hospitality for receiving me at the Baltic Nest Institute. Also many thanks to all the people of the Baltic Nest institute who made me feel welcome.

Crews and technicians onboard the HYPER/COMBINE cruise of May/June 2009 are acknowledged for their assistance, and Alf Norkko is thanked for provision of CTD data files. Laboratory assistance in Utrecht from Arnold van Dijk and Jan Drenth is greatly appreciated, and Wim the Boer at NIOZ. Many thanks to Miguel Rodriguez Medina at the Baltic Nest institute for extracting the data from the DAS data set.

Acknowledgements go to the institutes who gave permission to access their data in the BED database at Baltic Nest Institute, Stockholm University: Danish Institute for Fisheries and Marine Research (Hjalte Parner), Former Finnish Institute Marine Research (Riitta Olsonen), Baltic Sea Research Institute Warnemuende (Sabine Feistel), SMHIs Oceanografiska laboratorium (Jan Szaron and Lotta Fyrberg) and Russian State Hydrometeorological University St. Petersburg (Lev Karlin).

I appreciate the support and coaching of Koos during the process and also Anke and Anne. I would also like to thank Marieke Lammers for support and sharing her room with me, our discussions were not all fruitful but it greatly helped me to enjoy the process.

Finally, I want to deeply thank Hein van Heck, for his infinite support, faith and understanding.

References

- Alenius, P., Myrberg, K., and Nekrasov, A. (1998). The physical oceanography of the Gulf of Finland: a review. *Boreal Environment Research*, 3(2), 97-125.
- Algeo, T. J. and Ingall, E. (2007). Sedimentary Corg:P ratios, paleocean ventilation, and Phanerozoic atmospheric pO₂. *Palaeogeography, Palaeoclimatology, Palaeoecology*, 256(3), 130-155.
- Andrejev, O., Myrberg, K., Alenius, P. and Lundberg, P. A. (2004). Mean circulation and water exchange in the Gulf of Finland-a study based on three-dimensional modelling. *Boreal Environment Research*, 9(1), 1-16.
- Arneborg, L., Fiekas, V., Umlauf, L. and Burchard, H. (2007). Gravity current dynamics and entrainment-a process study based on observations in the Arkona Basin. *Journal of physical oceanography*, 37(8), 2094-2113.
- Balzer, W. (1982). On the distribution of iron and manganese at the sediment/water interface: thermodynamic versus kinetic control. *Geochimica et Cosmochimica Acta*, 46(7), 1153-1161.
- Berner, R. A. (1970). Sedimentary pyrite formation. *American Journal of Science*, 268(1), 1-23.
- Berner, R. A. (1984). Sedimentary pyrite formation: an update. *Geochimica et Cosmochimica Acta*, 48(4), 605-615.
- Boudreau, B. P. (1997). *Diagenetic models and their implementation* (Vol. 505). Berlin: Springer.
- Bray, J. T., Bricker, O. P. and Troup, B. N. (1973). Phosphate in interstitial waters of anoxic sediments: oxidation effects during sampling procedure. *Science*, 180(4093), 1362-1364.
- Cai, W. J. and Sayles, F. L. (1996). Oxygen penetration depths and fluxes in marine sediments. *Marine Chemistry*, 52(2), 123-131.
- Canfield, D. E. (1989). Reactive iron in marine sediments. *Geochimica et Cosmochimica Acta*, 53(3), 619-632.
- Canfield, D. E., Thamdrup, B. and Hansen, J. W. (1993). The anaerobic degradation of organic matter in Danish coastal sediments: Iron reduction, manganese reduction, and sulfate reduction. *Geochimica et Cosmochimica Acta*, 57(16), 3867-3883.
- Cardinale, M. and Modin, J. (1999). Changes in size-at-maturity of Baltic cod (*Gadus morhua*) during a period of large variations in stock size and environmental conditions, *Fish. Res.*, 41, 285-295.
- Chester, R. (2000). *Marine Geochemistry*, 2nd edition Blackwell.
- Claypool, G. E. Kaplan, IR (1974) The origin and distribution of methane in marine sediments. *Natural Gases in Marine Sediments*, Kaplan IR (ed.), Plenum Press, New York, NY, 99-139.
- Cloern, J. E. (2001). Our evolving conceptual model of the coastal eutrophication problem. *Marine ecology progress series*, 210(2001), 223-253.
- Conley, D. J., Humborg, C., Rahm, L., Savchuk, O. P. and Wulff, F. (2002). Hypoxia in the Baltic Sea and basin-scale changes in phosphorus biogeochemistry. *Environmental science & technology*, 36(24), 5315-5320.
- Conley, D. J., Björck, S., Bonsdorff, E., Carstensen, J., Destouni, G., Gustafsson, B. G., Hietanen, S., Kortekaas, M., Kuosa, H., Meier, H.E.M., Müller-Karulis, B., Nordberg, K., Norkko, A., Nürnberg, G., Pitkänen, H., Rabalais, N.N., Rosenberg, R., Savchuk, O.P., Slomp, C.P., Voss, M., Wulff, F. and Zillén, L. (2009). Hypoxia-related processes in the Baltic Sea. *Environmental Science & Technology*, 43(10), 3412-3420.

- Dellwig, O., Leipe, T., März, C., Glockzin, M., Pollehne, F., Schnetger, B., Yakushev, E.V., Böttcher, M.E. and Brumsack, H. J. (2010). A new particulate Mn–Fe–P-shuttle at the redoxcline of anoxic basins. *Geochimica et Cosmochimica Acta*, 74(24), 7100-7115.
- Diaz, R. J. and Rosenberg, R. (1995). Marine benthic hypoxia: A review of its ecological effects and the behavioural responses of benthic macrofauna, *Oceanogr. Mar. Biol.*, 33, 245–303.
- Diaz, R. J. and Rosenberg, R. (2008). Spreading dead zones and consequences for marine ecosystems. *science*, 321(5891), 926-929.
- Dickens, G. R. (2001). Sulfate profiles and barium fronts in sediment on the Blake Ridge: present and past methane fluxes through a large gas hydrate reservoir. *Geochimica et Cosmochimica Acta*, 65(4), 529-543.
- Einsele, W. (1936). Über die Beziehungen des Eisenkreislaufs zum Phosphatkreislauf im eutrophen See. *Arch. Hydrobiol*, 29(6), 664-686.
- Einsele, W. (1936): Über die Beziehungen des Eisenkreislaufs zum Phosphorkreislauf im eutrophen See, *Arch. Hydrobiol.*, 29, 664–686.
- Elken, J., Raudsepp, U. and Lips, U. (2003). On the estuarine transport reversal in deep layers of the Gulf of Finland. *Journal of Sea Research*, 49(4), 267-274.
- Elken, J. and Matthäus, W. (2008). Baltic Sea Oceanography. Regional Climate Studies, Assessment of climate change for the Baltic Sea Basin. Annex A, 1, 379-385.
- Emeis, K. C., Struck, U., Leipe, T., Pollehne, F., Kunzendorf, H. and Christiansen, C. (2000). Changes in the C, N, P burial rates in some Baltic Sea sediments over the last 150 years—relevance to P regeneration rates and the phosphorus cycle. *Marine Geology*, 167(1), 43-59.
- Feistel, R., Nausch, G., Matthäus, W. and Hagen, E. (2003). Temporal and spatial evolution of the Baltic deep water renewal in spring 2003. *Oceanologia*, 45(4).
- Fleming-Lehtinen, V., Laamanen, M., Kuosa, H., Haahti, H. and Olsonen, R. (2008). Long-term development of inorganic nutrients and chlorophyll α in the open northern Baltic Sea. *AMBIO: A Journal of the Human Environment*, 37(2), 86-92.
- Fonselius, S. H. (1969). In Fish board of Sweden (Ed.), *Hydrography of the baltic deep basins III*. (23rd ed.). Göteborg: Ser Hydrogr.
- Fonselius, S. (1981). Oxygen and hydrogen sulphide conditions in the Baltic Sea. *Marine pollution bulletin*, 12(6), 187-194.
- Fonselius, S. H., Szaron, J. and Öström, B. (1984). Long term salinity variations in the baltic sea deep water. *Publications of the International Council for the Exploration of the Sea* 185, pp.140-149.
- Froelich, P., Klinkhammer, G. P., Bender, M. A. A., Luedtke, N. A., Heath, G. R., Cullen, D., Dauphin, P., Hammond, D., Hartman, B. and Maynard, V. (1979). Early oxidation of organic matter in pelagic sediments of the eastern equatorial Atlantic: suboxic diagenesis. *Geochimica et Cosmochimica Acta*, 43(7), 1075-1090.
- Gustafsson, B. G. and Stigebrandt, A. (2007). Dynamics of nutrients and oxygen/hydrogen sulfide in the Baltic Sea deep water. *Journal of Geophysical Research: Biogeosciences* (2005–2012), 112(G2).
- Gustafsson, B. G., Schenk, F., Blenckner, T., Eilola, K., Meier, H.E.M., Müller-Karulis, B., Neumann, T., Ruoho-Airola, T., Savchuk, O.P. and Zorita, E. (2012). Reconstructing the development of Baltic Sea eutrophication 1850–2006. *Ambio*, 41(6), 534-548.
- Haapala, J. and Alenius, P. (1994). Temperature and salinity statistics for the northern Baltic Sea 1961–1990. *Finnish Marine Research*, 262, 51-121.

- Habicht, K. S. and Canfield, D. E. (1997). Sulfur isotope fractionation during bacterial sulfate reduction in organic-rich sediments. *Geochimica et Cosmochimica Acta*, 61(24), 5351-5361.
- Hansson, M., Andersson, L. and Axe, P. (2011). Areal extent and volume of anoxia and hypoxia in the Baltic Sea, 1960–2011. Report Oceanography, 42.
- HELCOM, (2013, nov): The nature of the Baltic Sea, http://helcom.navigo.fi/environment2/nature/en_GB/nature/
- HELCOM. (2007) The Baltic Sea Action Plan; Helsinki, Finland. <http://helcom.fi/baltic-sea-action-plan>
- HELCOM (2002) Environment of the Baltic Sea area 1994–1998. Baltic Sea environmental proceedings no. 82B.
- Helz, G. R., Miller, C. V., Charnock, J. M., Mosselmans, J. F. W., Patrick, R. A. D., Garner, C. D. and Vaughan, D. J. (1996). Mechanism of molybdenum removal from the sea and its concentration in black shales: EXAFS evidence. *Geochimica et Cosmochimica Acta*, 60(19), 3631-3642.
- Hille, S., Nausch, G. and Leipe, T. (2005). Sedimentary deposition and reflux of phosphorus (P) in the Eastern Gotland Basin and their coupling with P concentrations in the water column. *Oceanologia*, 47(4).
- Ingall, E. D., Bustin, R. M. and Van Cappellen, P. (1993). Influence of water column anoxia on the burial and preservation of carbon and phosphorus in marine shales. *Geochimica et Cosmochimica Acta*, 57(2), 303-316.
- Ingall, E. and Jahnke, R. (1994). Evidence for enhanced phosphorus regeneration from marine sediments overlain by oxygen depleted waters. *Geochimica et Cosmochimica Acta*, 58(11), 2571-2575.
- Jensen, H. S., Mortensen, P. B., Andersen, F. O., Rasmussen, E. and Jensen, A. (1995). Phosphorus cycling in a coastal marine sediment, Aarhus Bay, Denmark. *Limnology and Oceanography*, 908-917.
- Jilbert, T., Slomp, C. P., Gustafsson, B. G. and Boer, W. (2011). Beyond the Fe-P-redox connection: preferential regeneration of phosphorus from organic matter as a key control on Baltic Sea nutrient cycles. *Biogeosciences Discussions*, 8(1), 655-706.
- Jilbert, T. and Slomp, C. P. (2013a). Iron and manganese shuttles control the formation of authigenic phosphorus minerals in the euxinic basins of the Baltic Sea. *Geochimica et Cosmochimica Acta*, 107, 155-169.
- Jilbert, T. and Slomp, C. P. (2013b). Rapid high-amplitude variability in Baltic Sea hypoxia during the Holocene. *Geology*, 41(11), 1183-1186.
- Josefson, A. B., Norkko, J. and Norkko, A. (2012). Burial and decomposition of plant pigments in surface sediments of the Baltic Sea: role of oxygen and benthic fauna. *Marine Ecology Progress Series*, 455, 33-49.
- Jurva R. 1952a. Seas. In: Suomi, A general handbook on the geography of Finland. *Fennia* 72: 136–160.
- Karlson, K., Rosenberg R. and Bonsdorff, E. (2002). Temporal and spatial large-scale effects of eutrophication and oxygen deficiency on benthic fauna in Scandinavian and Baltic waters: a review. *Oceanography and Marine Biology*, 40, 427-489.
- Karlson, K., Hulth, S., Ringdahl, K. and Rosenberg, R. (2005). Experimental recolonisation of Baltic Sea reduced sediments: survival of benthic macrofauna and effects on nutrient cycling. *Marine Ecology Progress Series*, 294, 35-49.

- Kasten, S., Zabel, M., Heuer, V. and Hensen, C. (2004). Processes and signals of nonsteady-state diagenesis in deep-sea sediments and their pore waters. In *The South Atlantic in the Late Quaternary* (pp. 431-459). Springer Berlin Heidelberg.
- Klump, J. V. and Martens, C. S. (1981). Biogeochemical cycling in an organic rich coastal marine basin—II. Nutrient sediment-water exchange processes. *Geochimica et Cosmochimica Acta*, 45(1), 101-121.
- Kristensen, E., Kristiansen, K. D. and Jensen, M. H. (2003). Temporal behavior of manganese and iron in a sandy coastal sediment exposed to water column anoxia. *Estuaries*, 26(3), 690-699.
- Krom, M.D. and Berner, R.A. (1981). The diagenesis of phosphorus in a nearshore marine sediment. *Geochimica et Cosmochimica Acta*, 45(2), 207-216.
- Kullenberg, G. (1981). Physical oceanography. In A. Viopio (Ed.), *The Baltic sea*, Elsevier Oceanography Series, 30 ed., pp. 135-167.
- Larsson, U., Elmgren, R. and Wulff, F. (1985). Eutrophication and the Baltic Sea: causes and consequences. *Ambio*, 14.
- Lass, H. U. and Mohrholz, V., (2003). On dynamics and mixing of inflowings altwater in the Arkona Sea, *J. Geophys. Res.*, 108 (C2), 3042, doi: 10.1029/2002JC001465.
- Lukkari, K. (2008). Chemical characteristics and behaviour of sediment phosphorus in the northeastern Baltic Sea.
- Lukkari, K., Leivuori, M. and Kotilainen, A. (2009). The chemical character and behaviour of phosphorus in poorly oxygenated sediments from open sea to organic-rich inner bay in the Baltic Sea. *Biogeochemistry*, 96(1-3), 25-48.
- Lyons, T. W. and Severmann, S. (2006). A critical look at iron paleoredox proxies: New insights from modern euxinic marine basins. *Geochimica et Cosmochimica Acta*, 70(23), 5698-5722.
- MacKenzie, B., Hinrichsen, H. H., Plikshs, M., Wieland, K. and Zezera, A. S. (2000). Quantifying environmental heterogeneity: habitat size necessary for successful development of cod *Gadus morhua* eggs in the Baltic Sea. *Marine Ecology-Progress Series*, 193, 143-156.
- Mälkki, P. and Tamsalu, R. (1985). Physical features of the Baltic Sea. *Finnish Marine Research*. 252, 110 pp.
- März C., Hoffmann, J., Bleil, U., de Lange, G. J. and Kasten, S. (2008). Diagenetic changes of magnetic and geochemical signals by anaerobic methane oxidation in sediments of the Zambezi deep-sea fan (SW Indian Ocean). *Mar. Geol.* 255, 118–130.
- Matthäus, W. and Franck, H. (1992). Characteristics of major Baltic inflows—a statistical analysis. *Continental Shelf Research*, 12(12), 1375-1400.
- Mattäus, W. and Lass. H. U. (1995). The recent salt inflow into the baltic sea. *Journal of physical oceanography* 25, pp.280-286.
- McManus, J., Berelson, W. M., Coale, K. H., Johnson, K. S. and Kilgore, T. E. (1997). Phosphorus regeneration in continental margin sediments. *Geochimica et Cosmochimica Acta*, 61(14), 2891-2907.
- Meier, H. E. M., Feistel, R., Piechura, J., Arneborg, L., Burchard, H., Fiekas, V., Golenko, N., Kuzmina, N., Mohrholz, V., Nohr, C., Paka, V. T., Sellschopp, J., Stips, A. and Zhurbas, V. (2006). Ventilation of the baltic sea deep water: A brief review of present knowledge from observations and models. *Oceanologia* 48(S), pp.133-164.
- Meier, H. E. M. (2007). Modeling the pathways and ages of inflowing salt-and freshwater in the Baltic Sea. *Estuarine, Coastal and Shelf Science*, 74(4), 610-627.

- Middelburg, J. J. and Levin, L. A., (2009). Coastal hypoxia and sediment biogeochemistry. *Biogeosciences* 6, pp.1273-1293.
- Milucka, J., Ferdelman, T. G., Polerecky, L., Franzke, D., Wegener, G., Schmid, M., Lieberwirth, I., Wagner, M., Widdel, F. and Kuypers, M. M. (2012). Zero-valent sulphur is a key intermediate in marine methane oxidation. *Nature*, 491(7425), 541-546.
- Mort, H. P., Slomp, C.P., Gustafsson, B. G. and Andersen, T. J. (2010). Phosphorus recycling and burial in Baltic Sea sediments with contrasting redox conditions. *Geochimica et Cosmochimica Acta*, 74(4), 1350-1362.
- Mortimer, C. H. (1941). The exchange of dissolved substances between mud and water in lakes. *Journal of Ecology*, 29(2), 280-329.
- Mortimer, C. H. (1942). The exchange of dissolved substances between mud and water in lakes. *The Journal of Ecology*, 147-201.
- Nembrini, G. P., Capobianco, J. A., Viel, M. and Williams, A. F. (1983). A Mössbauer and chemical study of the formation of vivianite in sediments of Lago Maggiore (Italy). *Geochimica et Cosmochimica Acta*, 47(8), 1459-1464.
- Olsonen, R. (Ed.), (2007). FIMR Monitoring of the Baltic Sea environment – Annual report 2006. – Meri, Report Series of the Finnish Institute of Marine Research 59. – 58 p.
- Peketi, A., Joshi, R. K., Patil, D. J., Srinivas, P. L. and Dayal, A. M. (2012). Tracing the Paleo sulfate-methane transition zones and H₂S seepage events in marine sediments: An application of C-S-Mo systematics. *Geochemistry, Geophysics, Geosystems*, 13(10).
- Pitkänen, H., Lehtoranta, J. and Räike, A. (2001). Internal nutrient fluxes counteract decreases in external load: the case of the estuarial eastern Gulf of Finland, Baltic Sea. *AMBIO: A Journal of the Human Environment*, 30(4), 195-201.
- Reed, D. C., Slomp, C. P. and Gustafsson, B. G. (2011). Sedimentary phosphorus dynamics and the evolution of bottom-water hypoxia: A coupled benthic-pelagic model of a coastal system. *Limnology and Oceanography*, 56(3), 1075-1092.
- Reissman, J. H., Burchard, H., Feistel, R., Hagen, E., Lass, H. U., Mohrholz, V., Nausch, G., Umlauf, L. and Wieczorek, G., (2009). Vertical mixing in the baltic sea and consequences for eutrophication – A review. *progress in Oceanography* 82, pp.47-80.
- Reitz, A., Thomson, J., de Lange, G. J. and Hensen, C. (2006). Source and development of large manganese enrichments above eastern Mediterranean sapropel S1. *Paleoceanography*, 21(3).
- Rönnerberg, C. and Bonsdorff, E. (2004). Baltic Sea eutrophication: area-specific ecological consequences. *Hydrobiologia*, 514, 227-241.
- Rosenberg, R. (1990). Negative oxygen trends in Swedish coastal bottom waters. *Marine Pollution Bulletin*, 21(7), 335-339.
- Ruttenberg, K. C. (1992). Development of a sequential extraction method for different forms of phosphorus in marine sediments. *Limnology and Oceanography*, 37(7), 1460-1482.
- Ruttenberg, K. C. and Berner, R. A. (1993). Authigenic apatite formation and burial in sediments from non-upwelling, continental margin environments. *Geochimica et cosmochimica acta*, 57(5), 991-1007.
- Savchuk, O. P., Wulff, F., Hille, S., Humborg, C. and Pollehne, F. (2008). The Baltic Sea a century ago—a reconstruction from model simulations, verified by observations. *Journal of Marine Systems*, 74(1), 485-494.

- Schinke, H. and Matthäus, W. (1998). On the causes of major Baltic inflows--an analysis of long time series. *Continental Shelf Research*, 18(1), 67-97.
- Schulz, H. D., Dahmke, A., Schinzel, U., Wallmann, K. and Zabel, M. (1994). Early diagenetic processes, fluxes, and reaction rates in sediments of the South Atlantic. *Geochimica et Cosmochimica Acta*, 58(9), 2041-2060.
- Seeberg-Elverfeldt, J., Schluter, M., Feseker, T. and Kolling, M. (2005). Rhizon sampling of porewaters near the sediment-water interface of aquatic systems, *Limnol. Oceanogr.-Meth.*, 3, 361–371.
- Sellner, K. G. (1997). Physiology, ecology, and toxic properties of marine cyanobacteria blooms. *Limnology and Oceanography*, 42(5), 1089-1104.
- Shimmield, G. B. and Pedersen, T. F. (1990) The geochemistry of reactive trace metals and halogens in hemipelagic continental margin sediments. *Reviews in Aquatic Sciences*, 3, 255-279.
- Slomp, C. P., Van der Gaast, S. J. and Van Raaphorst, W. (1996). Phosphorus binding by poorly crystalline iron oxides in North Sea sediments. *Marine Chemistry*, 52(1), 55-73.
- Slomp, C. P., Epping, E. H., Helder, W. and Van Raaphorst, W. (1996b). A key role for iron-bound phosphorus in authigenic apatite formation in North Atlantic continental platform sediments. *Journal of Marine Research*, 54(6), 1179-1205.
- Slomp, C. P., Malschaert, J. F. P. and Van Raaphorst, W. (1998). The role of adsorption in sediment-water exchange of phosphate in North Sea continental margin sediments. *Limnology and Oceanography*, 43(5), 832-846.
- Slomp, C. P., Thomson, J. and de Lange, G. J. (2002). Enhanced regeneration of phosphorus during formation of the most recent eastern Mediterranean sapropel (S1). *Geochimica et Cosmochimica Acta*, 66(7), 1171-1184.
- Slomp, C. P., Mort, H. P., Jilbert, T., Reed, D. C., Gustafsson, B. G. and Wolthers, M. (2013). Coupled Dynamics of Iron and Phosphorus in Sediments of an Oligotrophic Coastal Basin and the Impact of Anaerobic Oxidation of Methane. *PloS one*, 8(4), e62386.
- Sohlenius, G., Emeis, K. C., Andrén, E., Andrén, T. and Kohly, A. (2001). Development of anoxia during the Holocene fresh-brackish water transition in the Baltic Sea. *Marine Geology*, 177(3), 221-242.
- Stigebrandt, A. (1987). A Model for the Vertical Circulation of the Baltic Deep Water. *Journal of Physical Oceanography*, 17(10), 1772-1785.
- Stumm, W. and Morgan, J. J. (2012). *Aquatic chemistry: chemical equilibria and rates in natural waters* (Vol. 126). John Wiley & Sons.
- Suikkanen, S., Laamanen, M. and Huttunen, M. (2007). Long-term changes in summer phytoplankton communities of the open northern Baltic Sea. *Estuarine, Coastal and Shelf Science*, 71(3), 580-592.
- Sundby, B., Gobeil, C., Silverberg, N. and Mucci, A. (1992). The phosphorus cycle in coastal marine sediments. *LIMNOLOGY*. Taylor, S. R. and McLennan, S. M. (1985). *The continental crust: its composition and evolution*.
- Thamdrup, B. (2000). Bacterial manganese and iron reduction in aquatic sediments. In *Advances in microbial ecology* (pp. 41-84). Springer US.
- Vahtera, E., Conley, D. J., Gustafsson, B. G., Kuosa, H., Pitkänen, H., Savchuk, O. P., Tamminen, T., Viitasalo, M., Voss, M., Wasmund, N. and Wulff, F. (2007). Internal ecosystem feedbacks enhance nitrogen-fixing cyanobacteria blooms and complicate management in the Baltic Sea. *AMBIO: A journal of the Human Environment*, 36(2), 186-194.

- Van Santvoort P. J. M., de Lange G., Thomson J., Colley S., Meysman F. and Slomp C. P. (2002) Oxidation and origin of organic matter in surficial Eastern Mediterranean hemipelagic sediments. *Aquat. Geochem.* 8, 153–175.
- Winterhalter, B. O. R. I. S., Flodén, T., Ignatius, H., Axberg, S. and Niemistö, L. (1981). Geology of the Baltic Sea. *The Baltic Sea*, 30, 1-121.
- Wulff, F. V., Rahm, L. A. and Larsson, P. (Eds.). (2001). *A systems analysis of the Baltic Sea* (Vol. 148). Springer.
- Zillén, L., Conley, D. J., Andrén, T., Andrén, E. and Björck, S. (2008). Past occurrences of hypoxia in the Baltic Sea and the role of climate variability, environmental change and human impact. *Earth-Science Reviews*, 91(1), 77-92